Journal: Ecological Applications

Manuscript Type: Article

Title: Joint species distribution modeling reveals a changing prey landscape for North Pacific right whales on the Bering shelf

Authors: Dana L Wright[1,2,3*], David G. Kimmel[4], Nancy Roberson[5], and David Strausz[2,6]

[1]Duke University Marine Laboratory, Beaufort, NC, USA

[2]University of Washington, Cooperative Institute for Climate, Ocean, and Ecosystem Studies, Seattle, WA, USA

[3]NOAA, Marine Mammal Laboratory, Seattle, WA, USA

[4]NOAA, Alaska Fisheries Science Center, Seattle, WA, USA

[5]NOAA, Resource Assessment and Conservation Engineering Division, Seattle, WA, USA

[6]NOAA, Pacific Marine Environmental Laboratory, Seattle, WA, USA

**Contact author and corresponding author: dana.wright@duke.edu*

Open Research Statement: Zooplankton abundance data for all species included in our study are stored in the Dryad Repository Wright et al. (2023), https://doi.org/10.5061/dryad.hqbzkh1nn. Bottom water and surface water temperature data are available via the R package coldpool https://github.com/afsc-gap-products/coldpool by querying coldpool::coldpool and exporting years 2005 to 2017. Climate indices and ice cover are available for download from the Bering Climate website at https://www.beringclimate.noaa.gov/data/index.php by querying Aleutian Low, North Pacific, DPO, West Pacific, Arctic Osc., and ice retreat for 2005 to 2017. If the website is down, these

data are available by contacting the webmaster email address on the aforementioned website. Ice retreat was derived from sea ice satellite data downloaded from Comiso, J.C. (2017) Bootstrap Sea Ice Concentrations from Nimbus-7 SMMR and DMSP SSM/I-SSMIS, Version 3 [Data Set]. Boulder, Colorado USA. NASA National Snow and Ice Data Center Distributed Active Archive Center. https://doi.org/10.5067/7Q8HCCWS4I0R. Wind direction and wind gust variables were derived from satellite data downloaded from Hersbach, H., Bell, B., Berrisford, P., Biavati, G., Horányi, A., Muñoz Sabater, J., Nicolas, J., Peubey, C., Radu, R., Rozum, I., Schepers, D., Simmons, A., Soci, C., Dee, D., Thépaut, J-N. (2023): ERA5 hourly data on single levels from 1940 to present. Copernicus Climate Change Service (C3S) Climate Data Store (CDS), DOI: 10.24381/cds.adbb2d47. 2019 GEBCO bathymetry data were downloaded from GEBCO Gridded Bathymetry Data at https://www.gebco.net/data_and_products/gridded_bathymetry_data/ by querying WMS for GEBCO 2019 grid under Previous Releases. This submission does not use novel code. Reproducible steps to use each R and ArcGIS Pro package that we used in our analysis are included in the *Methods* and Appendix S1: Section S2, to Appendix S1: Section S4 sections of the manuscript.

Keywords: Bering Sea; *Calanus glacialis;* cold pool; community ecology; ecosystem management; *Eubalaena japonica*; food web; IUCN Red list; joint species distribution model; population dynamics; zooplankton

Abstract

The eastern North Pacific right whale (NPRW) is the most endangered population of whale and has been observed north of its core feeding ground in recent years with low sea ice extent. Sea ice and water temperature are important drivers for zooplankton dynamics within the whale's core feeding ground in the southeastern Bering Sea, seasonally forming stable fronts along the shelf that give rise to distinct zooplankton communities. A northward shift in NPRW distribution driven by changing distribution of prey resources could put this species at increased risk of entanglement and vessel strikes. We modeled the abundance of NPRW prey, *Calanus glacialis, Neocalanus,* and *Thysanoessa* species, using a dynamic biophysical food web model of nine zooplankton guilds in the Bering shelf zooplankton community during a period of warming (2006-2016). This model is unique from prior zooplankton studies from the region in that it includes density dependence, thereby allowing us to ask whether species interactions influence zooplankton dynamics. Modeling confirmed the importance of sea ice and ocean temperature to zooplankton dynamics in the region. Density-independent growth drove community dynamics while dependent factors were comparatively minimal. Overall, *Calanus* responded to environment terms, with the strength and direction of response driven by copepodite stage. *Neocalanus* and *Thysanoessa* responses were weaker, likely due to their primary occurrence on the outer shelf. We also modeled the steady-state (equilibrium) abundance of *Calanus* in conditions with and without wind gusts to test whether advection of outer shelf species might disrupt steady-state dynamics of *Calanus* abundance; results did not support disruption. Given the annual fall sampling design, we interpret our results as follows: low-ice extent winters induced stronger spring winds and weakened fronts on the shelf, thereby advecting some outer shelf species into the study region; increased development rates in these warm conditions

influenced the proportion of *C. glacialis* copepodite stages over the season. Residual correlation suggests missing drivers, possibly predators and phytoplankton bloom composition. Given the continued loss of sea ice in the region and projected continued warming, our findings suggest that *C. glacialis* will move northward, and thus, whales may move northward to continue targeting them.

Introduction

The core feeding ground of the critically endangered remnant population of eastern North Pacific right whale (NPRW; *Eubalaena japonica*) is on the southeastern Bering Sea shelf (SEBS; Figure 1, Shelden et al., 2005; Zerbini et al., 2015). NPRWs have been recently observed north of their SEBS core feeding ground during low ice extent years (Filitova et al., 2019; Stabeno & Bell, 2019; Wright et al., 2019; Matsuoka et al., 2021). In the Atlantic Ocean, the congener North Atlantic right whale (*Eubalaena glacialis;* NARW) has recently expanded range (Crowe et al., 2022), which has been attributed to decreasing prey on primary foraging grounds driven by climate (Record et al., 2019; Meyer-Gutbrod et al., 2022). A northward shift by NPRWs towards the Bering Strait, a vessel chokepoint, driven by shifts in prey resources could put this species at increased risk of vessel strikes and entanglement given the projected increase in trans-Arctic shipping and contracted species ranges resulting from the accelerating loss of sea ice (Bringham, 2010; Smith et al., 2013; Dawson et al., 2018; Stevenson & Lauth 2019; Fedewa et al. 2020).

The 500 km wide SEBS is comprised of three stable oceanographic Domains derived from seasonal sea ice – Inner (0-50 m isobath), Middle (50-100 m isobath), and Outer (100-200 m isobath; Coachman 1986) – each with distinct water masses that have similar zooplankton communities (Stabeno et al., 2012a; Eisner et al., 2014). Specifically, sinking spring meltwater

from the sea-ice creates a cold pool (<2 ºC) on the bottom of the Middle Domain that persists on the shelf until fall mixing (Stabeno et al., 2012a). This cold pool acts as a hydrographic barrier, influencing distribution and trophic dynamics across the shelf. For example, the cold pool is a refugia for zooplanktivorous age-0 walleye pollock (*Gadus chalcogrammus*) from piscovorous age 2+ pollock, which are mainly concentrated on the Outer Domain (Wyllie-Echeverria & Wooster, 1998; Kotwicki et al., 2005; Mueter & Litzow 2008). In addition, the cold pool has been a northward barrier to the northern Bering Sea until the anomalous warm year of 2018 when sea ice did not extend into the Bering Sea at all (Stabeno et al., 2012b; Duffy-Anderson et al., 2019; Huntington et al., 2020).

This cold pool typically has aggregations of the large lipid-rich copepod *Calanus marshallae*/*glacialis* (termed *C. glacialis* here considering recent genetic information; Tarrant et al., 2021), a central forage species for a myriad of zooplanktivores in this system, including NPRWs (Omura et al., 1969; Baumgartner et al., 2013). Community variability in zooplankton composition and abundance in this region is well described (Napp et al., 2002; Coyle et al., 2008; Ohashi et al., 2013; Eisner et al., 2015, 2018). Fluctuations in the sea ice extent and resulting cold pool has been shown to correlate to shifts in the diet composition of zooplanktivores on the shelf, with less large zooplankton (lipid rich copepods and euphausiids) consumed by age-0 pollock and Pacific cod (*Gadus macrocephalus*) during warm bottom water conditions (Buckley et al., 2016; Farley et al., 2016). Warm conditions have also correlated with zooplanktivore seabird die-offs (Baduini et al. 2001, Jones et al. 2019).

The motivation to better understand this complex food web has resulted in extensive research, yet, few studies include density dependence, which would allow us to ask whether species interactions influence prey dynamics. Competition for resources may increase among

zooplankton during warm periods as ice retreat impacts phytoplankton dynamics (bloom timing and bloom composition; Leu et al., 2011; Sigler et al., 2016). These dynamics were most recently conceptualized in Kimmel et al. (2018), which proposes that an absence of spring ice algae will cause *C. glacialis* to feed later in the spring on microzooplankton in a warmer water column, altering development rates of life stages (Hirst et al., 2003), species interactions, and predation within the zooplankton community.

The objective of the present study was to model the Bering Shelf zooplankton community using a dynamic biophysical food web model (gjamTime; Clark et al. 2020) during a period of climate variability (2006-2016) to study the population dynamics of potential prey of NPRWs. Specifically, we estimated the influence of sea ice, the cold pool, ocean temperature and wind variables on the density-independent growth responses and density-dependent interactions of species in the zooplankton community. Further, we estimated the net effects of density-independent and dependent factors (i.e., species interactions) on steady-state (i.e., equilibrium) abundances of right whale prey species. These equilibrium abundances were predicted in conditions with and without wind gusts to test whether advection of outer shelf species might disrupt *Calanus* steady-state abundance across a gradient in bottom water temperature. We hypothesized that the abundance of *C. glacialis* will correlate positively with increased prevalence of cold bottom water as has been shown in prior studies (Napp et al., 2002; Coyle et al., 2008, Søreide et al., 2010; Kimmel et al., 2018). We also hypothesized that *C. glacialis* would develop faster in low ice extent conditions (Hirst et al., 2003; Sigler et al. 2016, Kimmel et al. 2018). Further, we hypothesized that dependent factors (i.e., species interactions) would influence the dynamics of right whale prey species (Hunt et al., 2011; Kimmel et al., 2018). Finally, we hypothesized that advection of outer shelf *Neocalanus* and *Thysanoessa* species

would impact the steady-state abundance of *Calanus* copepodite stages (Campbell et al. 2016; Hunt et al. 2016). Understanding the prey dynamics of the rare eastern NPRW may help to predict future changes in foraging effort and distribution that could place it at risk of adverse interactions with human activities.

Methods

North Pacific right whale prey species

We defined the potential prey for NPRW in our study of the Bering shelf to include *C. glacialis*, *Neocalanus* species, and *Thysanoessa* species, hereafter referred to as potential prey, based on stomach content, tagging, and visual observation studies (Omura et al., 1969; Wade et al., 2011b; Baumgartner et al. 2013; Ford et al., 2016). *C. glacialis* in the Bering Sea aggregates on the Middle Domain of the SEBS, and exhibits a one-year life cycle with one cohort developing from nauplii through copepodite stages over the summer months before accumulating enough lipids to enter diapause by early fall (Cooney & Coyle, 1982, Smith & Vidal, 1986; Napp et al., 2002; Coyle et al., 2008). *Thysanoessa raschii* is a Middle Domain euphausiid believed to continuously reproduce over the summer season (Smith, 1991; Pinchuk & Coyle, 2008; Hunt Jr. et al., 2016). In contrast, *Thysanoessa inermis* and *Thysanoessa spinifera* are found primarily on the Outer Domain while *Thysanoessa longipes* occurs in deeper waters off the shelf (Smith, 1991; Hunt et al., 2016). *Neocalanus cristatus* and *Neocalanus* spp. (*Neocalanus flemingeri* and *Neocalanus plumchrus*) are also traditionally Outer Domain species that enter diapause by late June after reproducing in late spring (Smith & Vidal, 1986; Vidal & Smith, 1986; Napp et al., 2002).

Study Area and Species Data

We selected the 70 m isobath on the eastern Bering shelf (~56.5°N to 62.5°N; Figure 2) from 2006 – 2016, as our study region to maximize the spatial and temporal coverage of the Middle Domain and Bering Sea right whale critical habitat with available zooplankton data during a period of overall warming.

Zooplankton species abundance (ind. m^{-3}) were obtained from fall cruises (mid-August – early October) on the Bering shelf from 2006 to 2016. Zooplankton were collected using oblique tows of paired bongo nets (20 cm diameter frame with 153 μm mesh, and a 60 cm diameter frame with 333 or 505 μm mesh; Incze et al., 1997; Napp et al., 2002). These oblique tows spanned from ~10 m of the bottom to the surface from a boat moving at ~1.5 knots. Net depth was determined using a SeaCat or FastCat conductivity, temperature, and depth (CTD) sensor (Sea-Bird Electronics), and the volume filtered was estimated using a General Oceanics flowmeter mounted inside the mouth of each net. Onboard, zooplankton samples were preserved in formalin for later laboratory sorting and identification. Plankton were processed using an established splitting and subsampling protocol (e.g., Coyle et al., 2008; Kimmel et al., 2018) and were identified to the lowest taxonomic level and stage possible at the Plankton Sorting and Identification Center (Szczecin, Poland), and verified at the Alaska Fisheries Science Center, Seattle, Washington, USA. It is important to note that euphausiid abundances reported here are semi-quantitative as larger euphausiids are able to avoid capture (Sameoto et al., 1993). Accurate and precise measurements of euphausiid abundances in the Bering Sea remain the subject of debate (Hunt Jr. et al., 2016). Given the similar methodology in capturing euphausiids over time in the dataset, we included these abundance estimates in our analysis as relative indicators of euphausiid populations on the Bering Shelf.

Because of unequal sampling effort for zooplankton and environmental data over the study region, we averaged zooplankton tow data and environmental variables to a study grid comprised of fourteen contiguous 80 km^2 cells (Figure 2) for each time-step. The cell size was chosen to maximize cell number while maintaining contiguity along the isobath; the grid shapefile was created using the *Grid Index Features* tool on a polygon in ArcGIS Pro (v 2.5). To maximize our assemblage, our models used samples (including species, size classes, and stages) that were collected using consistent sampling methodology over the time-series and occurred at least five times in the dataset (Clark et al., 2017). Sizes and stages were summed for a given species or genus to reach the five-occurrence threshold over the study period where appropriate using R statistical software (R Core Team 2020) package *dplyr* (v 1.0.0; Wickham et al., 2020). This resulted in a multivariate dependent dataset comprised of the abundance of 20 individual species classified into a total of 41 size classes and stages (Figure 3, Appendix S1: Table S1) for each of the 14 grid squares at each time-step (2006-2016).

Model

We chose the dynamic biophysical food web model gjamTime (Clark et al., 2020) to model the zooplankton community because this framework includes density independent (DI) growth responses and density dependent (DD) interactions through 'environmental-species interactions' terms (ESI), defined as biotic and abiotic factors that propagate through food webs and impact community dynamics. The gjamTime model links the hierarchical Bayesian joint attribute model gjam (Clark et al. 2017; see Appendix S1: Section S2 for description) to an extended generalized Lotka Volterra (LV) model of a species' rate of change, S, defined as:

$$\frac{dw_s}{dt} = w_s(\rho_s + \sum_{s'}^{S} \alpha_{s,s'} w_{s'}) \quad \text{(Equation 1)}$$

where w_s is the abundance of the focal species and ρ_s is the rho term, and thus, w_s*ρ_s is the DI rate of change of the focal species. The second term, $\alpha_{s,s'}w_{s'}$, is the DD rate of change, depending on the abundance of the non-focal species $w_{s'}$ and its interaction effect with the focal species $\alpha_{s,s'}$ for all species from *s'* to *S*. The LV model often includes a third constant term that does not depend on w_s; this term is often used to describe migration/emigration.

The gjamTime model extends the LV model by including ESIs in three terms:

$$\frac{dw_s}{dt} = x'\boldsymbol{\beta}_s + (w_s \times x')\boldsymbol{\rho}_s + (w_s \times w')\boldsymbol{\alpha}_s + \varepsilon_s \qquad \text{(Equation 2)}$$

where the first term ($x'\boldsymbol{\beta}_s$) represents the migration/emigration term of the LV model, the second term $(w_s \times x')\boldsymbol{\rho}_s$ represents DI growth, and the third term $(w_s \times w')\boldsymbol{\alpha}_s$ represents DD. gjamTime includes a fourth term, ε_s which represents the model error in the form of an S × S covariance matrix. The first term is defined as a vector of coefficients $\boldsymbol{\beta}_s$ (betas) describing the response to environmental variables in a vector x. We will use the label 'movement' for this term instead of migration/emigration to follow the language in Clark et al. (2020). For the second term, referred to as rho, gjamTime extends LV by allowing for interactions between population abundance (w_s) and environment (x) in DI growth [$(w_s \times x')$]. The gjamTime model also extends the third term by allowing DD interactions [$(w_s \times w')$], with w representing all species in the community. The DD matrix $\boldsymbol{\alpha}_s$ (alpha) is a prior for the model, allowing for interactions between individual species at each discrete time-step (-1 for negative, 0 for neutral, and 1 for positive interactions), thereby incorporating food web theory into the model (see Appendix S1: Section S2 for further details). There is one Equation 2 for each species, thus coefficient vectors $\boldsymbol{\beta}$ (beta), $\boldsymbol{\rho}$ (rho), and $\boldsymbol{\alpha}$ (alpha) become matrices of S rows (denoted with bold). The resulting model is a discrete-time dynamic biophysical model. The gjamTime framework has been

successfully applied to terrestrial and freshwater lake systems (e.g., Clark et al., 2020; Collins et al., 2022).

Density-dependent species matrix

We structured the planktonic community for the $\boldsymbol{\alpha_s}$ species matrix based on size and trophic relationship. A species assemblage diagram is shown in Figure 3. Nine zooplankton guilds were defined using the World Register of Marine Species (https://www.marinespecies.org/), the Biodiversity of Marine Plankton Copepods (Razouls et al., 2022), the Northern GOA LTER (https://nga.lternet.edu/), and primary literature (Brodsky, 1950; Grainger, 1961, Mauchline, 1965, Corkett & McLaren, 1989; Miller et al., 1984). We defined a community of small (< 1.2 mm) omnivores dominated by *Pseudocalanus* spp., small copepodite stages of *Metridia* spp., and small copepodite stages of *C. glacialis* (Figure 2). Also in the small category are adult *Acartia* spp. and Euphausiid nauplii. Euphausiid nauplii are not identified to species and join the small category due to their size and are not considered NPRW prey. Small-medium omnivores (1.2-3.5 mm) included larger stages of *C. glacialis* as well as *Metridia pacifica*, small life history stages of *Neocalanus* spp., *Mysidae*, *Limacina helicina*, and Euphausiid (calyptopis stage). Euphausiid calyptopis stages are not identified to species. Medium-large omnivores (3.5-10 mm) consisted of larger stages of *Neocalanus cristatus, Eucalanus bungii,* and *Neocalanus* spp. Large omnivores (>10 mm) included juvenile and adult *Thysanoessa* spp. and Decapoda. Four guilds of predators were also defined, consisting of Chaetognaths and Cnidaria with size classes < 5 mm, 5-20 mm, and >20 mm. Finally, we defined an epibenthic community consisting of Amphipods and Ostracods < 5 mm and a microzooplankton predator community consisting of *Oithiona* spp. from life history stages copepodite C5 and Adult. Note that for each species, there is intra-

specific competition as well as inter-specific competition within the guild in addition to predator-prey linkages (denoted by arrows in the figure). As mentioned previously, interaction priors are coded as 1 (positive), 0 (non-interaction), and -1 (negative) in the $\boldsymbol{\alpha_s}$ matrix.

Environmental data

We selected environmental variables for DI growth and movement terms based on prior studies of zooplankton communities in the North Pacific and subarctic (Napp et al., 2002, Coyle et al., 2008; 2011; Ohashi et al., 2013; Eisner et al., 2014; Kimmel et al., 2018; Thorson et al., 2019). The full list of potential variables is in Appendix S1: Table S2, and how each variable was derived is described in Appendix S1: Section S3. To limit redundancy in environmental data, variables were limited to those having correlation < |0.7| (Dormann et al., 2013; Appendix S1: Figure S1) with priority given to variables that have been significant to Bering Sea zooplankton community structure in prior analyses and whose values varied over the spatial grid. As DI growth and movement terms are separate terms in the model (Equation 2), and thus computed independently, correlations between these terms were ignored.

Resulting DI terms to be used in model fitting included *in situ* bottom (BT) and surface temperature (ST; Table 1), as temperature has a strong effect on the growth rate of zooplankton species (Hirst et al., 2003). Movement terms included cold pool extent (pCP – a derived cold pool measure of the percentage of cold pool per grid square for each study grid square at each time-step), ice extent (IE), number of days with ice after March 15th (iDm), seasonal wind direction (NWs = summer northwesterly winds, NWw = winter northwesterly winds, SEs = summer southeasterly winds; SEw = winter southeasterly winds;), wind gusts (WGs = summer, WGf = fall, WGw = winter, and WGsp = spring), and the oceanographic index, the Aleutian

Low (AL; Table 1). We also included Latitude to explore spatial effects. Estimates of phytoplankton abundance using chlorophyll *a* concentrations were not used in the analysis as chlorophyll *a* data were not consistently collected on all surveys used in the analysis. Also, *in situ* salinity data were not included in the model as not all data were publicly available due to delays in QA/QC of these data. We excluded these two variables to prevent spatial and temporal bias in the model.

Modeling and Model Selection

Model fitting was performed using the Markov chain Monte Carlo (MCMC) technique Gibbs sampling. To define relationships between environmental variables and NPRW prey species, we fit models using the same dependent data comprised of all zooplankton species with different combinations of environmental terms, and compared the fitted models using Deviance Information Criterion (DIC). By including all species in the model, we leveraged the joint attribute model framework to model population dynamics of our target species (NPRW prey). DIC is a model selection criterion appropriate for Bayesian models computed with MCMC techniques with normal posterior distributions. Like Akaike Information Criterion (AIC), smaller DIC values are preferred as DIC penalizes by the effective number of parameters as well as the model deviance However, given the multivariate framework of a JSDM, DIC provides a metric to determine the best model of the zooplankton community. In other words, the lowest DIC model will reflect the subset of species who respond strongest to the included variables. Because of this, individual species that responds strongly to a subset of variables could drive model selection. Consequently, while DIC guided our model selection, we ultimately defined the best model using model predictions of potential right whale prey (*C. glacialis, Neocalanus* species,

295 and *Thysanoessa* species) with priority given to *C. glacialis* as the primary prey type of SEBS
296 right whales (Appendix S1: Figure S5).

297 For all models, zooplankton abundance was fourth root transformed to improve model
298 fitting, because of the high range in abundance within the dataset (zero to tens of thousands). The
299 global model consisted of DI growth ($\boldsymbol{\rho}$) terms BT and ST and movement ($\boldsymbol{\beta}$) terms pCP, Lat,
300 IE, IDm, SEs, NWs, SEw, NWw, WGs, WGw, WGsp, WGf, AL (full variable names are
301 provided in Table 1) and interactions of pCP and Lat (pCP*Lat) and SEs and Lat (SEs*Lat).
302 Priors and effort are defined in Appendix S1: Section S4. The model output is an abundance
303 estimate for each species at each grid square. Because the scale of the predictors varied
304 dramatically (a few ºC to thousands of km^2), we standardized large-scale variables prior to model
305 fitting using z-scores: IE, Lat, WGs, WGw, WGsp, WGf, pCP*Lat, and SEs*Lat. The global
306 model and iterations of reduced models were computed using the wind gust threshold of >10 m/s
307 and >15 m/s and compared using DIC.

308 During model fitting, a total of 15% of missing zooplankton data were imputed using the
309 gjamTime function *gjamFillMissingTimes,* including all grid cells for 2013 because zooplankton
310 sampling did not occur in the Bering Sea that year (Appendix S1: Figure S4). There were no
311 missing environmental data. Fitted models for model comparison were ran with all zooplankton
312 species using one chain for 20,000 iterations and a burn-in of 5,000 in the R package *gjam* (v
313 2.3.2; Clark et al., 2020). The selected best model, defined as the model that best predicted *C.*
314 *glacialis* (Appendix S1: Figure S5*)*, was run with one chain for 50,000 iterations and 5,000 burn-
315 in. We adopted the diagnostic approach of sequentially doubling the iterations and inspecting
316 chains for convergence (Collins et al., 2022) and using the diagnostic plots in the *gjam* R
317 package to assess model fit (Appendix S1: Section S5) as is recommended by the model

architects (Clark et al., 2017, 2020) and used in prior studies using gjamTime (e.g., Collins et al. 2022).

Equilibrium abundance

The supplemental gjamTime function *wrapperEquilAbund* provided a framework to investigate if inclusion of movement (i.e., migration/emigration) into the model framework would impact the steady-state (i.e., equilibrium) abundance of *C. glacialis* over a gradient in bottom water temperature. We chose bottom water temperature because of its significance to our model and prior studies on *C. glacialis* from the region (e.g., Coyle et al., 2008; 2011; Hunt Jr. et al., 2011; 2018; Eisner et al. 2014; Kimmel et al., 2023). We hypothesized the inclusion of movement would impact the steady-state abundance by both allowing *C. glacialis* to move out of the study region and allow advection of potential competitor outer shelf large-bodied species (*Neocalanus* and *Thysanoessa*) into the study region under warm ocean conditions (Campbell et al., 2016; Hunt et al., 2016).

To test our hypothesis, we used *wrapperEquilAbund* to model the net effect of density independent and dependent factors on the equilibrium abundance (**w***) of *C. glacialis* over a gradient in bottom water temperature for gjamTime model outputs with and without movement terms (spring and fall wind gusts; Table 2). Thus, we ran two gjamTime models, one model with DI growth (bottom and surface temperature) and movement terms (spring and fall wind gusts; Table 2) and one model with only DI growth terms. Each gjamTime model was ran for one chain with 20,000 iterations and 5,000 burn-in; chains were inspected for convergence. For both model outputs, we simulated 2,000 equilibrium abundance values (**w***) on the model output scale (fourth-root transformed) for each species over a bottom water temperature gradient (zero-

centered spanning two standard deviations) using *wrapperEquilAbund* and calculated predictive intervals across the gradient. Because the distribution of equilibrium abundances was drawn from the posterior distribution, convergence is not required. It is important to note that these equilibrium abundances offer a benchmark for comparison; we are not assuming or arguing that any species is at equilibrium.

Intuitively, the *wrapperEquilAbund* algorithm is asking a high-dimensional version of Robert M. 'Bob' May's ecological question, 'can two species coexist in a given habitat?' (May 1975). Because gjamTime uses discrete time and is an expanded LV model, assuming $\frac{dw_s}{dt} = 0$ of Equation 2 at sequential time-steps would indicate steady-state (carrying capacity). Therefore, the *wrapperEquilAbund* algorithm seeks to find an abundance, **w***, for all species simultaneously given a gjamTime model output that sets $\frac{dw_s}{dt} = 0$ over a chosen environmental gradient in the model. The simulation keeps the other model predictors (environmental terms) constant, thereby optimizing the abundance in a specific environment. Because only linear responses are provided in the gjamTime framework, this simulation can test whether dependent factors influence steady state abundance as a nonlinear response is only induced indirectly from differential species responses to the gradient. This algorithm has successfully predicted species interactions observed in a closed lake system and provided insight into species interactions in an open system of migratory birds (Clark et al. 2020). Nevertheless, our data are comprised of species with short life history strategies that include multiple sampled stages (e.g., copepodite stages of *C. glacialis* over one summer), and thus, our *wrapperEquilAbund* results may reflect cohorts with different development rates as well as movement (migration/emigration) with species interactions.

Results

Models with ice, cold pool extent, *in situ* temperature, and wind gust terms performed better than models with wind direction and oceanographic indices (Table 2). In addition, all models with wind gust threshold >15 m/s performed better than models with >10 m/s. The best model of the zooplankton community, defined as the model with the lowest DIC, consisted of DI growth terms bottom (BT) and surface temperature (ST), and movement terms sea ice extent (IE), spring and fall wind gusts (WGsp and WGf, respectively), and the percentage of cold pool per grid square (pCP). The best model prioritizing NPRW prey, defined as the most that best predicted *C. glacialis*, consisted of DI growth terms BT and ST, and movement terms WGsp and WGf (Table 2; Appendix S1: Figure S7).

Zooplankton Assemblage Dynamics

DI growth contributed the most to community dynamics of the zooplankton species assemblage followed by movement, which was variable within and among species (Figure 4). In general, movement contributed more to species found traditionally on the Outer Domain and off shelf environments (e.g., *T. inermis*, *T. spinifera*, *T. longipes*, *Neocalanus*, *Metrididae*) and was smallest for omnipresent small omnivores, *Pseudocalanus* and *Oithiona* spp. The contribution of DD to community dynamics was minimal across the assemblage but, in general, decreased with increasing size class of zooplankton. This trend was reflected in the copepodite stages of *C. glacialis* but was nominal for all stages of *Neocalanus* dynamics. For *Thysanoessa* species, DD contributed the most to *T. inermis* followed by *T. raschii*, *T. longipes*, and finally *T. spinifera* (Figure 4).

In general, relationships between rho (DI growth) and beta (movement) terms were stronger for *C. glacialis* than *Neocalanus* or *Thysanoessa* (Figure 5; Appendix S1: Section S6).

Out of the copepodite stages for *C. glacialis*, only C3 and C4 had significant relationships (defined as >95% of the posterior distribution away from zero) with bottom temperature (both negative). A significant relationship with surface temperature was negative for older stages of *C. glacialis* (C5 and Adult) and positive for C3. For *Neocalanus*, only Adult *Neocalanus* spp. responded significantly to any DI growth (rho) term (negative response to surface temperature). Similarly, only *T. raschii* responded significantly to DI growth (negative with bottom temperature), although, in general, species trended in the same response direction (Figure 5a).

Overall, few species showed a significant relationship to the movement (beta) terms (Figure 5b). For *C. glacialis*, C2 had no relationship with either variable. The remaining stages had a negative relationship to spring wind gusts, while C3 and C4 had a significant relationship with fall wind gusts (negative). For *Thysaneossa* species, *T. inermis* responded significantly (positive with spring wind gusts). Both C5 *N. cristatus* and C5 *Neocalanus* spp. responded to beta terms, with *N. cristatus* responding negatively to spring wind gusts and *Neocalanus* spp. responding negatively to fall wind gusts (Figure 5b; Appendix S1: Section S6).

Steady-state abundance

General trends in the shape of predicted equilibrium abundance of *C. glacialis* copepodite stages over a gradient in bottom water temperature did not differ between models that included the movement terms of spring and fall wind gusts and a model of only DI growth terms bottom and surface temperature (Figure 6). Equilibrium abundance estimates were lower for the model without movement terms, and nonlinear responses varied with copepodite stage. In addition, the trend in C3 and C4 shifted to a more multimodal shape for the model without movement terms,

while the maximum equilibrium abundance of Adult *C. glacialis* became more pronounced at mid bottom temperature.

Across models, the highest predicted abundance for C2, C3, and C5 stages occurred at higher bottom temperature. In contrast, the highest C4 and Adult abundance was predicted at intermediate bottom water temperature. Predicted equilibrium abundance trends of *Neocalanus* and *Thysaonessa* species for the movement model are provided in Appendix S1: Figure S9.

Discussion

Zooplankton assemblage dynamics were dominated by DI growth, specifically *in situ* bottom and surface temperature, emphasizing the critical role that temperature plays in zooplankton community dynamics (Hirst et al. 2003). In addition, movement terms – sea ice extent, cold pool, and wind gusts – were significant to the community. Our results reinforce prior studies that found sea ice and the cold pool significant to the Bering shelf zooplankton community (Coyle & Pinchuk 2002; Stabeno et al., 2012a; Duffy-Anderson et al., 2017; Thorson et al., 2019; 2020; Kimmel et al. 2023) adding credence to the utility of this modeling approach to model zooplankton dynamics.

In contrast to our hypothesis, however, sea ice and cold pool variables were not significant variables to the best model of *C. glacialis*. Instead, resulting lower temperatures and stronger winds from reduced ice years influenced population dynamics of this species. Our modeling results suggest lower abundance of *C. glacialis* and higher abundance of *T. raschii* and *T. inermis* in low ice conditions. We propose the reason for the predicted shift in species composition in our study region is due to spring wind gusts during low ice conditions advecting traditionally Outer Domain species (*T. inermis*) into the study region (i.e., onto the Middle

Domain) from temperature-induced weakened fronts between the Domains and wind gusts delaying water column stability that supports the spring bloom of *C. glacialis.* In concert, the warm temperatures have implications for development rates and lipid storage of *C. glacialis* and *T. raschii* on the shelf. Together, our results suggest a community-scale shift in zooplankton abundance resulting from ice dynamics, with some species responding directly to the reduced ice extent whereas others are responding to shifts in oceanographic and atmospheric dynamics from the ice absence. This combined with the minimal observed density dependence across the community underpin that all zooplankton in the community are likely to be ultimately driven by temperature effects on their biology, which is heavily influenced by the annual ice regime and cold pool extent.

Zooplankton Assemblage Dynamics

Community dynamics were dominated by DI growth with minimal contribution of dependent factors (DD). DD was most important for small omnivores (<1.2 mm), likely reflecting their omnipresence, overall high abundance, and life history strategy of multiple cohorts within a season. Weak DD across the assemblage does not mean that DD does not occur, only that it can be a weak predictor of abundances in a subsequent year given the sampling design and life history of these species. In contrast to other systems such as migratory birds with site fidelity, an individual adult *C. glacialis* sampled in one year is a different animal from a distinct cohort compared with an adult *C. glacialis* collected in the prior year. Weakly informed species interactions have been observed in terrestrial open systems using gjamTime (Clark et al., 2020). In addition, the gjamTime state-space model framework does not include rate parameters such as specifically defined growth rates or mortality due to predation, which are important factors when

455 describing predator-prey dynamics of zooplankton communities (Leu et al., 2011, Brun et al.,
456 2016).

457 Notably, DD decreased with increasing life history stage of *C. glacialis*. We believe this
458 trend combined with the DI results reflects temperature-driven development rates of life history
459 stages of *C. glacialis* over the summer – smaller life stages had positive responses to colder
460 bottom temperatures whereas larger life stages had positive responses to colder surface
461 temperatures. Given the one-year life cycle of *C. glacialis* on the shelf, our results support prior
462 work that *C. glacialis* grows slower in colder water conditions, resulting in more small size class
463 individuals in the water column during the fall sampling period and greater opportunity to
464 observe lipid rich C5 stages in the fall (Hunt Jr. et al., 2002, 2011; Coyle et al., 2008, 2011;
465 Sigler et al., 2016; Kimmel et al., 2018).

466 In contrast to *C. glacialis*, *Neocalanus* and *Thysanoessa* species exhibited overall weak to
467 absent relationships to DI growth and movement terms, except for *T. raschii*, *T. inermis*, and late
468 stage *Neocalanus* species. *T. raschii*, a species believed to reproduce continuously over the
469 summer season in the Middle Domain (Smith, 1991; Pinchuk & Coyle, 2008; Hunt Jr. et al.,
470 2016), exhibited a positive growth response to bottom temperature, likely reflecting faster
471 development and reproductive rates in warm water conditions, similar to *C. glacialis*. While not
472 significant, other *Thysanoessa* species trended toward a positive growth rate with DI terms.
473 Additionally, the negative growth response of Adult *Neocalanus spp.* to surface temperature
474 could be attributed to pressure-induced advection driven by temperature and pressure gradients
475 between the cold pool water mass and warmer Outer Domain waters in large ice extent
476 conditions.

Excluding *T. raschii, Neocalanus* and *T. inermis* are traditionally Outer Domain species, with small frequency in our dataset, likely influencing the poor model fit (Appendix S1: Figure S6). Additionally, as mentioned previously, euphausiid abundances reported here are semi-quantitative as larger euphausiids can avoid capture, and therefore, abundance estimates of *Thysanoessa* species in our analysis are relative indicators of euphausiid populations given the similar methodology in capturing euphausiids over time in the dataset. Therefore, the euphausiid data likely reflect trends over time and space, but that the exact abundances are not known with precision. That said, all results for *T. longipes* should be interpreted cautiously because this is an off-shelf species that rarely occurs in the study region.

The contribution of movement to the model dynamics was variable across the zooplankton assemblage. The small proportion described for small omnivores, likely reflects their high abundance throughout the study region (Kimmel et al., 2018). Outside of the smallest guild, movement was variable within and among species, possibly reflecting differential transport of zooplankton species in water masses depending on life history strategy (i.e., diapause and diel vertical migration). For example, *Thysanoessa* species are strong diurnal vertical migrators whereas only larger *C. glacialis* stages diel migrate vertically (Schabetsberger et al., 2000; Baumgartner et al., 2013; Hunt Jr. et al. 2016). This could possibly explain why fall winds only affected smaller stages of *C. glacialis*. This contrasts with spring wind gusts, which were inversely correlated with most stages of *C. glacialis*; we propose this relationship is explained by advection and vertical mixing of *C. glacialis* in the wind-mixed surface layers as they spawn and develop in late spring into summer. Together, these results support that *C. glacialis* populations tend to accumulate under stable water column conditions and thus are available for capture during fall surveys.

However, the contribution of movement to a given species' dynamics occurred for multiple species with weak or absent relationships to wind variables via the posterior predictions (Figures 4, 5). This apparent mismatch could be due to a joint response of species in the model to species and environmental covariates not included in the model. In other words, a missing common predator or prey item or environmental predictor of covarying species could be reflected as movement in the model. Cascading trophic connections on the eastern Bering Shelf and their interplay with the environment are conceptualized in the Oscillating Control Hypothesis (OCH; Hunt Jr. et al., 2002; 2011; Coyle et al., 2011). In the OCH, early life stages of walleye pollock are a key predator of zooplankton in the Bering Sea. In addition, multiple seabirds target large mesozooplankton on the Bering Shelf (Hunt Jr. et al., 2018). Our model did not include predators believed to provide top-down influence in the system. Similar responses to shared prey resources excluded from the model, such as phytoplankton or microzooplankton, could also be reflected in the movement term. Spring ice algae is believed to be important to the life history of *C. glacialis* (Søreide et al., 2010; Leu et al., 2011; Banas et al., 2016; Kimmel et al., 2018). The residual correlation plot from our model supports the hypothesis of missing predator and/or prey items, as high correlation in residual variation was observed among some zooplankton species believed to drive trophic dynamics of the OCH, including *C. glacialis* (Appendix S1: Figure S8; Hunt et al., 2011; Kimmel et al., 2018). Inclusion of multifarious data (e.g., fish counts and algal biomass) to our current model is possible in the gjamTime framework and recommended to further quantify community dynamics in this system.

Equilibrium Abundance

The predicted steady state (equilibrium) abundance analysis further supports our conclusion that DI growth and movement terms reflect temperature-induced plasticity in development rate and bloom timing as well as advection of *C. glacialis* driven by sea-ice dynamics. Overall, linear trends were observed for C2 and C3 stages, confirming more early-stage animals in the water column at fall sampling from a delayed spring bloom. In addition, general trends did not change when movement terms were excluded from the model, suggesting advection of Outer Domain species onto the Middle Shelf is not dramatically influencing steady-state dynamics of *C. glacialis*. Yet, as mentioned previously, predation and grazing rates are not included in this model framework. Nevertheless, the multimodal shape of some *C. glacialis* stages suggests species interactions given the algorithm models environment linearly across species. The predicted equilibrium abundance is a net effect of density independent and density dependent effects from the model output, and thus, as noted above, the results reflect cohort development rates as well as movement (for models with beta terms) with species interactions. Thus, the late-stage *C. glacialis* results could reflect increased competition for prey resources for C5 at lower bottom temperatures, and increased competition for C4 and Adult stages at higher temperatures. Alternatively, these results could reflect increased predation on copepodite stages by chaetognaths and cnidaria or a combination of delayed spring bloom dynamics with faster development through stages and earlier diapause under warm water conditions.

Yet another potential occurrence that relates to reduced ice cover is that the observed trends reflect two overlapping generations in the fall sampling. Banas et al. (2016) proposed that the number of cohorts for a *Calanus* species in a geographic location are driven by prey phenology and temperature. The equilibrium abundance trends hint at the idea that a second cohort may be produced in warm conditions where the first cohort develops quickly and puts

energy into egg production, while the second cohort invests in lipid production for diapause, resulting in an overlap of individuals in development (e.g., C2, C3) and preparing for diapause (e.g., C5) at the time of sampling. While intriguing, essential ecological questions remain regarding the plausibility of a two-cohort strategy. Many papers have argued the importance of prey phenology, mainly the presence of spring sea ice algae, to the success of *C. glacialis* on the Bering shelf (Søreide et al., 2010; Banas et al., 2016). Nevertheless, *C. glacialis* was found in our study during years and areas that did not have widespread spring sea ice. Furthermore, *C. glacialis* have been observed on the Outer Domain in low ice years (Hunt Jr. et al., 2018). Consequently, there may be unknown plasticity of *C. glacialis* egg development in the Bering Sea – two distinct haplotypes of *C. glacialis* exist in the Bering Sea and Arctic (Nelson et al., 2009). Alternatively, the individuals collected in low-ice years may be the morphologically similar species *Calanus marshallae*, which might not rely as heavily on spring ice algae. Indeed, the ability to morphologically distinguish between *C. finmarchicus* and *C. glacialis* in the north Atlantic appears to be impossible without the use of DNA markers (Choquet et al., 2018).

It's worth noting that a myriad of additional factors that likely influence steady-state dynamics of *C. glacialis* were not included in either model framework, but our results support that inclusion of DI growth and movement terms capture some of the variability and trends in *C. glacialis* dynamics that have been attributed to ice dynamics and development rates in prior work (Napp et al., 2002, Coyle et al., 2008; Campbell et al., 2016; Kimmel et al., 2018).

Implications for North Pacific right whales

Understanding population dynamics of potential right whale prey may help to predict future changes in right whale distribution. If *C. glacialis* shifts northward with the retreating ice to stay

568 in cold bottom water conditions, right whales may track their movement to continue feeding on
569 their preferred prey. Recent detections of right whales in the northern Bering Sea in low ice
570 extent years support that at least some whales are moving north to find adequate prey patches on
571 the Bering Shelf (Filatova et al., 2019; Stabeno & Bell, 2019; Wright et al., 2019). Alternatively,
572 the advection of Outer Domain genera (*T. inermis*) and increase in growth rate of Middle
573 Domain *T. raschii* as suggested by our models may support NPRW on the SEBS grounds during
574 low ice extent years, but it is unclear based on our study when Outer Domain species are being
575 advected and whether enough biomass is advected to support feeding right whales and the
576 myriad of other zooplanktivores on the Middle Domain, many of which are not as mobile as
577 large cetaceans. Our model also hints that *C. glacialis* may transition to a two-cohort strategy on
578 the Middle Domain in warm conditions, which may supplement the advected Outer Domain
579 biomass. Under the two-cohort scenario, right whales may be able to target late stage
580 copepodites of *C. glacialis* earlier in the foraging season, although the proportion and energy
581 density of late-stage animals in the upper water column over the season is unknown.
582 Importantly, our model only included data up to 2016. Ice has continued to retreat in the
583 Arctic following the years of our study, including an absence of ice in the Bering Sea during the
584 winter of 2017-18 (Stabeno & Bell 2019). In the following summer, calanoids and euphausiids
585 had 14% less lipids compared with high ice-extent years (Duffy-Anderson et al., 2019) and the
586 zooplankton community shifted to smaller, lipid poor species (Kimmel et al., 2023), suggesting
587 that whales may need to consume more individual prey items in low ice conditions, which could
588 impact foraging effort and targeted prey patch sizes. A 2018 research cruise documented right
589 whales in the southern and northern Bering Sea within a two-week period of July (Matsuoka et
590 al., 2021) suggesting either a range expansion to find adequate prey as was proposed by prior

591 tagging work (Zerbini et al., 2015) or a transition to individual foraging strategies. Photographs
592 from the NPRW catalogue suggest that individuals are currently in good body condition (Amy
593 Kennedy, University of Washington, pers. comm.). Nevertheless, forecasts of biophysical
594 models predict the Bering shelf bottom waters may warm by 5 °C by 2100 (Hermann et al.,
595 2019).

596 A northward shift or expansion to continue feeding on *C. glacialis* could put NPRWs at
597 higher risk for ship-strike given projected marine traffic in the region, especially near the Bering
598 Strait chokepoint (Smith et al., 2013, Hauser et al., 2018, Silber & Adams 2019). In addition,
599 various fishery species in the Bering Sea are shifting north outside of the SEBS, which has been
600 attributed to the reduced ice extent (Stevenson & Lauth 2019, Fedewa et al., 2020).
601 Entanglement in fishing gear and ship-strike are concerning threats for NPRW conservation as
602 these threats are the primary cause of mass mortality of the congener NARW in the past three
603 decades (Knowlton et al., 2012, Sharp et al., 2019). While an entanglement has never been
604 observed for NPRW, a presumed eastern NPRW was photographed with scars consistent with
605 entanglement (Ford et al., 2016). In addition, multiple western North Pacific right whales show
606 evidence of entanglement (Burdin et al., 2004) and bowhead whales (*Balaena mysticetus*) in the
607 Northern Bering Sea have been entangled in snow crab (*Chionoecetes opilio*) gear (Brownell,
608 1999); this gear type has lethally entangled congener North Atlantic right whales (Davies &
609 Brillant 2019). The remote Alaska region makes it unlikely entanglements of NPRW are
610 observed given the majority of urban NARW entanglements are missed (NOAA Fisheries 2021).

611 In summary, NPRWs are exceptionally difficult to study given their rarity, but our results
612 shed light on community structure of their prey items during a period of warming. The recent
613 rapid reduction in sea ice on the primary feeding ground of NPRWs is impacting population

dynamics of potential right whale prey (Kimmel et al., 2023, this study) and conditions will continue to warm (Hermann et al., 2019). A northward shift by NPRWs to continue feeding on *C. glacialis* could put this species at increased risk of entanglement and ship strike as well as raises questions regarding impacts to the energy budget and life history of these rare whales. Consequently, further monitoring of the distribution, abundance, and health of NPRWs and their prey items is critical.

Acknowledgements

We thank the Commanding Officers, officers, and crews of the numerous research vessels that have conducted the research surveys as well as the Zakład Sortowania I Oznaczania Planktonu in Szczecin, Poland, for identifying copepods. We also thank AFSC-RACE Groundfish Assessment Program survey participants for the bottom and surface temperature collections, Dr. James Clark for his assistance in modeling and reviewing the manuscript, and Dr. Andy Read for comments on the manuscript. This analysis was funded by the North Pacific Research Board Graduate Research Fellowship, the NSF Graduate Research Fellowship Program, and the Duke University Graduate Student Training Enhancement Grant.

Conflict of Interest Statement: The authors do not believe there are any real or perceived conflicts of interest regarding this research. This work conforms to the legal requirements of the country in which it was carried out (USA).

References

Arctic Council. 2009. “Arctic Marine Shipping Assessment Report 2009.” 194 pp.

637 Arrigo, K.R. & van Dijken, G.L. 2004. “Annual changes in sea-ice, chlorophyll a, and primary
638 production in the Ross Sea, Antarctica.” *Oceanography* 51: 117-138.
639 Baier, C.T., & Napp, J.M. 2003. “Climate-induced variability in *Calanus marshallae*
640 populations.” *Journal of Plankton Research* 25(7): 771-782.
641 Banas, N.S., Moller, E.F., Nielson, T.G., and Eisner, L.B. 2016. “Copepod life strategy and
642 population viability in response to prey timing and temperature: Testing a new model
643 across latitude, time, and the size spectrum.” *Frontiers in Marine Science* 3: 225.
644 Baumgartner, M.F., and Mate, B.R. 2003. “Summertime foraging ecology of North Atlantic right
645 whales.” *Marine Ecology Progress Series* 264: 123-135.
646 Baumgartner, M.F., Lysiak N.S.J., Esch, H.C., Zerbini, A.N., Berchok, C.B., and Clapham, P.J.
647 2013. “Associations between North Pacific right whales and their zooplanktonic prey in
648 the southeastern Bering Sea.” *Marine Ecology Progress Series* 490: 267–284.
649 Bringham, L.W. 2010. “The fast-changing maritime Arctic.” *Proceedings of the U.S. Naval*
650 *Institute* 136: 55–59.
651 Brodsky, K. A. 1950. Calanoida of the far eastern seas and polar basins of the USSR. Israel
652 Program for Scientific Translations, 1967. 440 pp. (Original: Keys to the Fauna of the
653 USSR, No. 35, Akademia Nauk SSSR)
654 Brownell, R. L., Jr. 1999. “Mortality of a bowhead whale in fishing gear in the Okhotsk Sea.”
655 Paper SC/51/AS28 presented to the Scientific Committee of the IWC, unpublished.
656 Available for the IWC office in Cambridge, UK.
657 Brueggeman, J. J., R. A. Grotefendt and A. W. Erickson. 1984. “Endangered whale abundance
658 and distribution in the Navarin Basin of the Bering Sea during the ice-free period.” Pages
659 201–236 in B. R. Melteff and D. H. Rosenberg, eds. Proceedings of the Workshop on

660 Biological Interactions Among Marine Mammals and Commercial Fisheries in the
661 Southeastern Bering Sea, University of Alaska Sea Grant Report 84-1.
662 Brun, P., Payne, M.R. and Kiørboe, T., 2016. Trait biogeography of marine copepods–an
663 analysis across scales. *Ecology Letters 19*(12): 1403-1413.
664 Buckey, T.W., Ortiz, I., Kotwicki, S., and Aydin, K. 2016. Summer diet composition of walleye
665 pollock and predator-prey relationships with copepods and euphausiids in the eastern
666 Bering Sea, 1987-2011." *Deep-Sea Research Part II: Topical Studies in Oceanography*
667 134: 302-311.
668 Burdin, A.M., Nikulin, V.S. and Brownell Jr, R.L. 2004. "Cases of entanglement of western
669 North-Pacific right whales (Eubalaena japonica) in fishing gear: serious threat for species
670 survival." *Marine mammals of the Holarctic. KMK Scientific Press, Moscow, Russia*
671 pp.95-97.
672 Campbell, R.G., Ashjian, C.J., Sherr, E.B., Sherr, B.F., Lomas, M.W., Ross, C., Alatalo, P.,
673 Gelfman, C., and Keuren, D.V. 2016. "Mesozooplankton grazing during spring sea-ice
674 conditions in the eastern Bering Sea." *Oceanography* 134: 157–171.
675 Choquet, M., Kosobokova, K., Kwasniewski S., Hatlebakk, M., Dhanasiri, A.K.S., Melle, W.,
676 Daase, M., Svensen, C., Soreide, J.E., and Hoarau. G. 2018. "Can morphology reliably
677 distinguish between the copepods *Calanus finmarchicus* and *C-glacialis*, or is DNA the
678 only way?" *Limnology and Oceanography-Methods* 16: 237-252.
679 Clapham, P.J., A.S. Kennedy, B.K. Rone, A.N. Zerbini, J.L. Crance, and C.L. Berchok. 2012.
680 North Pacific right whales (*Eubalaena japonica*) in the southeastern Bering Sea. Final
681 Report. OCS Study BOEM 2012-074. National Marine Mammal Laboratory, Alaska
682 Fisheries Science Center, NOAA. 175pp.

683 Clark, J.S., Nemergut, D., Seyednasrollah, B., Turner, P., and Zhang. S. 2017. “Generalized joint
684 attribute modeling for biodiversity analysis: Median-zero, multivariate, multifarious
685 data.” *Ecological Monographs* 87: 34–56.
686 Clark, J.S., Scher, C.L. and Swift, M. 2020. “The emergent interactions that govern biodiversity
687 change.” *Proceedings of the National Academy of Sciences* 117(29): 17074–17083.
688 Corkett, C.J., and McLaren, I.A. 1978. “The biology of *Pseudocalanus”*, p. 1-231. *In*: Russell,
689 F.S. and Yonge, M. (eds.), *Advances in Marine Biology* 15.Cooney, R.T., and Coyle,
690 K.O. 1982. “Trophic implications of cross-shelf copepod distibutions in the Southeastern
691 Bering Sea.” *Marine Biology* 70: 187-196.
692 Collins, C.G., Elmendorf, S.C., Smith, J.G., Shoemaker, L., Szojka, M., Swift, M. and Suding,
693 K.N., 2022. Global change re-structures alpine plant communities through interacting
694 abiotic and biotic effects. *Ecology Letters*, *25*(8): 1813-1826.
695 Coyle, K.O., & Pinchuk, A.I. 2002. “Climate-related differences in zooplankton density and
696 growth on the inner shelf of the southeastern Bering Sea.” *Progress in Oceanography* 55:
697 177-194.
698 Coyle, K.O., Pinchuk, A.I., Eisner, L.B., and Napp, J.M. 2008. “Zooplankton species
699 composition, abundance, and biomass on the eastern Bering Sea shelf during summer:
700 The potential role of water-column stability and nutrients in structuring the zooplankton
701 community.” *Deep-Sea Research II* 55: 1775–1791.
702 Coyle, K.O., Eisner, L.B., Mueter, F.J., Pinchuk, A.I., Janout, M.A., Cieciel, K.D., Farley, E.V.,
703 and Andrews, A.G. 2011. “Climate changes in the southeastern Bering Sea: impacts on
704 pollock stocks and implications for the oscillating control hypothesis.” *Fisheries*
705 *Oceanography* 20(2): 139–156.

706 Crowe, L.M., Brown, M.W., Corkeron, P.J., Hamilton, P.K., Ramp, C., Ratelle, S., Vanderlaan,
707 A.S. and Cole, T.V. 2021. “In plane sight: a mark-recapture analysis of North Atlantic
708 right whales in the Gulf of St. Lawrence.” *Endangered Species Research 46*: 227-251.
709 Dalpadado, P., Arrigo, K.R., van Dijken, G.L., Skjoldal, H.R., Bagøein, E., Dolgov, A.V.,
710 Prokopchuk, I.P., and Sperfeld, E. 2020. “Climate effects on temporal and spatial
711 dynamics of phytoplankton and zooplankton in the Barents Sea.” *Progress in*
712 *Oceanography* 185: 102320.
713 Daoust, P.-Y., E.L. Couture, T. Wimmer, and L. Bourque. 2017. “Incident Report: North
714 Atlantic Right Whale Mortality Event in the Gulf of St. Lawrence, 2017.” Collaborative
715 Report produced by Canadian Wildlife Health Cooperative, Marine Animal Response
716 Society, Fisheries and Oceans Canada, 224 pp.
717 Davies, K.T.A., and Brillant, S.W. 2019. “Mass human-caused mortality spurs federal action to
718 protect endangered North Atlantic right whales in Canada.” *Marine Policy* 104: 157–162.
719 Davies, K.T.A., Brown, M.W., Hamilton, P.K., Knowlton, A.R., Taggart, C.T., and Vanderlaan,
720 A.S.M. 2019. Variation in North Atlantic right whale *Eubalaena glacialis* occurrence in
721 the Bay of Fundy, Canada, over three decades.” *Endangered Species Research* 39: 159–
722 171.
723 Dawson, J., Pizzolato, L., Howell, S.E.L., Copland, L., and Johnston, M.E. 2018. “Temporal and
724 spatial patterns of ship traffic in the Canadian Arctic from 1990 to 2015.” *Arctic* 71(1):
725 15–28.
726 Dormann C. F., Elith J., Bacher S., Buchmann C., Carl, G., Carré, G., García Marquéz, J.R.,
727 Gruber, B., Lafourcade, B., Leitão, P.J., Munkemüller, T., McClean, C., Osborne, P.E.,
728 Reineking, B., Schröder, B., Skidmore, A.K., Zurell, D., and Lautenbach, S. 2013.

"Collinearity: a review of methods to deal with it and a simulation study evaluating their performance." *Ecography* 36: 27–46.

Duffy-Anderson, J.T., Stabeno, P., Andrews III, A.G., Cieciel, K., Deary, A., Farley, E., Fugate, C., Harpold, C., Heintz, R., Kimmel, D., Kuletz, K. 2019. "Responses of the northern Bering Sea and southeastern Bering Sea pelagic ecosystems following record-breaking low winter sea ice." *Geophysical Research Letters* 46(16): 9833–9842.

Eisner, L.B., Napp, J.M., Mier, K.L., Pinchuk, A.I., and Andrews, A.J. III. 2014. "Climate-mediated changes in zooplankton community structure for the eastern Bering Sea." *Deep-Sea Research II* 109: 157–171.

Eisner, L.B., Siddon, E.C. and Strasburger, W.W., 2015. "Spatial and temporal changes in assemblage structure of zooplankton and pelagic fish in the eastern Bering Sea across varying climate conditions." *TINRO 181*: 141-160.

Eisner, L.B., Pinchuk, A.I., Kimmel, D.G., Mier, K.L., Harpold, C.E. and Siddon, E.C., 2018. "Seasonal, interannual, and spatial patterns of community composition over the eastern Bering Sea shelf in cold years. Part I: zooplankton." *ICES Journal of Marine Science 75*(1): 72-86.

Fedewa, E.J., Jackson, T.M., Richar, J.I., Gardner, J.L. and Litzow, M.A. 2020. "Recent shifts in northern Bering Sea snow crab (*Chionoecetes opilio*) size structure and the potential role of climate-mediated range contraction." *Deep Sea Research Part II: Topical Studies in Oceanography 181*: 104878.

Filatova, O.A., Fedutin, I.D., Titoa, O.V, Meschersky, I.G., Ovsyanikova, E.N. Antipin, M.A., Burdin, A.M., and Hoyt, E. 2019. "First encounter of the North Pacific right whale (*Eubalaena japonica*) in the waters of Chukotka." *Aquatic Mammals* 45(4): 425–429.

752 Ford, J.K.B., Pilkington, J.F., Gisborne, B., Frasier, T.R., Abernethy, R.M., and Ellis, G.M.
753 2016. “Recent observations of critically endangered North Pacific right whales
754 (*Eubalaena japonica*) off the west coast of Canada.” *Marine Biodiversity Records* 9: 50.
755 Fossheim, M., Primicerio, R., Johannesen, E., Ingvaldsen, R.B., Aschan, M.M., and Dolgov,
756 A.V. 2015. “Recent warming leads to a rapid borealization of fish communities in the
757 Arctic.” *Nature Climate Change* 5: 673- 678.
758 Grainger, E. H. 1961. “The copepods *Calanus glacialis* (Jaschnov) and *CaIanus finmarchicus*
759 (Gunnerus) in Canadian Arctic-Subarctic waters.” *Journal of Fisheries Research Board*
760 *Canada* 18: 663-678.
761 Hauser, D.D., Laidre, K.L. and Stern, H.L. 2018. “Vulnerability of Arctic marine mammals to
762 vessel traffic in the increasingly ice-free Northwest Passage and Northern Sea
763 Route.” *Proceedings of the National Academy of Sciences 115*(29): 7617-7622.
764 Hermann, A.J., Gibson, G.A., Cheng, W., Ortiz, I., Aydin, K., Wang, M., Hollowed, A.B.,
765 Holsman, K.K., and Sathyendranath, S. 2019. “Projected biophysical conditions of the
766 Bering Sea to 2100 under multiple emission scenarios.” *ICES Journal of Marine Science*
767 76: 1280-1304.
768 Hirst, A. G., and Bunker, A. J. 2003. Growth of marine planktonic copepods: global rates and
769 patterns in relation to chlorophyll *a*, temperature, and body weight. Limnology and
770 Oceanography, 48: 1988-2010.
771 Hunt, G.L. Jr., Stabeno, P., Walters, G., Sinclair, E., Brodeur, R.D., Napp, J.M., and Bond, N.A.
772 2002. “Climate change and control of the southeastern Bering Sea pelagic ecosystem.”
773 *Deep-Sea Research II* 49: 5281–5853.

774 Hunt, G.L. Jr., Stabeno, P.J., Strom, S., Napp, J.M. 2008. “Patterns of spatial and temporal
775 variation in the marine ecosystem of the southeastern Bering Sea, with special reference
776 to the Pribilof Domain.” *Deep-Sea Research Part II: Topical Studies in Oceanography*
777 55: 1919-1944.
778 Hunt, G.L. Jr., Coyle, K.E., Eisner, L.B., et al. 2011. “Climate impacts on eastern Bering Sea
779 foodwebs: a synthesis of new data and an impact of the Oscillating Control Hypothesis.”
780 *ICES Journal of Marine Science* 68: 1230–1243.
781 Hunt Jr., G. L., Ressler, P. H., Gibson, G. A., De Robertis, A., Aydin, K., Sigler, M. F., Ortiz, I.,
782 et al. 2016. “Euphausiids in the eastern Bering Sea: A synthesis of recent studies of
783 euphausiid production, consumption and population control.” *Deep-Sea Research Part II*
784 *Topical Studies in Oceanography* 134: 204-222.
785 Hunt, G.L., Jr., Renner, M., Kulettz, K.J., Salo, S., Eisner, L., Ressler, P.H., Ladd, C., and
786 Santora, J.A. 2018. “Timing of sea-ice retreat affects the distribution of seabirds and their
787 prey in the southeastern Bering Sea.” *Marine Ecology Progress Series* 593: 209–230.
788 Huntington, H.P., Daniel, R., Hartsig, A., Harun, K., Heiman, M., Meehan, R., Noongwook, G.,
789 Pearson, L., Prior-Parks, M., Robards, M., and Stetson, G. 2015. “Vessels, risks, and
790 rules: Planning for safe shipping in Bering Strait.” *Marine Policy* 15: 119-127.
791 Huntington, H.P., Danielson, S.L., Wiese, F.K., Baker, M., Boveng, P., Citta, J.J., De Robertis,
792 A., Dickson, D.M.S., Farley, E., George, J.G., Iken, K., Kimmel, D.G., Kuletz, K., Ladd,
793 C., Levine, R., Quakenbush, L., Stabeno, P., Stafford, K.M., Stockwell, D., and Wilson,
794 C. 2018. “Evidence suggests potential transformation of the Pacific Arctic ecosystem is
795 underway.” *Nature Climate Change* 10: 342-348.

796 Huntington, H.P., Bobbe, S., Hartsig, A., Knight, E.J., Knizhinikov, A., Moiseev, A.,
797 Romanenko, O., Smith, M.A., and Sullender, B.K. 2019. “The role of areas to be avoided
798 in the governance of shipping in the greater Bering Strait region.” *Marine Policy* 110:
799 103564.
800 Kimmel, D.G., Eisner, L.B., Wilson, M.T., et al. 2018. “Copepod dynamics across warm and
801 cold periods in the eastern Bering Sea: Implications for walleye pollock (*Gadus*
802 *chalcogrammus*) and the Oscillating Control Hypothesis.” *Fisheries Oceanography* 27:
803 143–158.
804 Knowlton, A.R., Hamilton, P.K., Marx, M.K., Pettis, H.M. and Kraus, S.D. 2012. “Monitoring
805 North Atlantic right whale *Eubalaena glacialis* entanglement rates: a 30 yr
806 retrospective.” *Marine Ecology Progress Series 466*: 293-302.
807 Laist, D.W., Knowlton, A.R. and Pendleton, D. 2014. “Effectiveness of mandatory vessel speed
808 limits for protecting North Atlantic right whales.” *Endangered Species Research, 23*(2):
809 133-147.
810 Leu, E., Søreide, J.E., Hessen, D.O., Falk-Petersen, S. and Berge, J., 2011. Consequences of
811 changing sea-ice cover for primary and secondary producers in the European Arctic shelf
812 seas: timing, quantity, and quality. *Progress in Oceanography*, *90*(1-4): 18-32.
813 Liu, N., Lin, L., Wang, Y., Chen, H., and Yan, H.E. 2016. “The distribution and inter-annual
814 variation of water masses on the Bering Sea shelf in summer.” *Acta Oceanologica Sinica*
815 35(11): 59-67.
816 Matsuoka, K., Crance, J.L., Taylor, J.K.D., Yoshimura, I., James, A., and An, Y. 2021. “North
817 Pacific right whale (*Eubalaena japonica*) sightings in the Gulf of Alaska and the Bering

Sea during IWC-Pacific Ocean Whale and Ecosystem Research (IWC-POWER) surveys." *Marine Mammal Science* DOI: 10.1111/mms.12889.

Mauchline, J. 1965. "The larval development of the euphausiid, *Thysanoessa raschii* (M. Sars). *Crustaceana* 9(1): 31-40.

May, R.M., 1975. Biological populations obeying difference equations: stable points, stable cycles, and chaos. *Journal of Theoretical Biology*, *51*(2), pp.511-524.

Mellinger, D.K., Moore, S.E., Munger, L., and Fox, C.G., 2004. "Detection of North Pacific right whale (*Eubalaena japonica*) calls in the Gulf of Alaska." *Marine Mammal Science* 20(4): 872-879.

Meyer-Gutbrod, E.L., Davies, K.T., Johnson, C.L., Plourde, S., Sorochan, K.A., Kenney, R.D., Ramp, C., Gosselin, J.F., Lawson, J.W. and Greene, C.H. 2022. "Redefining North Atlantic right whale habitat-use patterns under climate change." *Limnology and Oceanography*. https://doi.org/10.1002/lno.12242

Miller, C.B., Frost, B.W., Batchelder, H.P., Clemons, M.J., and Conway, R.E. 1984. "Life histories of large, grazing copepods in a subarctic ocean gyre: *Neocalanus plumchrus*, *Neocalanus cristatus*, and *Eucalanus bungii* n the Northeast Pacific." *Progress in Oceanography* 13(2): 201-243.

Møller, E.F., and Nielson, T.G. 2020 "Borealization of Arctic zooplankton – smaller and less fat zooplankton species in Disko Bay, Western Greenland. *Limnology and Oceanography* 65: 1175-1188.

Muto, M. M., V. T. Helker, B. J. Delean, N. C. Young, J. C. Freed, R. P. Angliss, N. A. Friday, P. L. Boveng, J. M. Breiwick, B. M. Brost, M. F. Cameron, P. J. Clapham, J. L. Crance, S. P. Dahle, M. E. Dahlheim, B. S. Fadely, M. C. Ferguson, L. W. Fritz, K. T. Goetz, R.

C. Hobbs, Y. V. Ivashchenko, A. S. Kennedy, J. M. London, S. A. Mizroch, R. R. Ream, E. L. Richmond, K. E. W. Shelden, K. L. Sweeney, R. G. Towell, P. R. Wade, J. M. Waite, and A. N. Zerbini. 2021. 2021. "Alaska Marine Mammal Stock Assessments, 2020." U.S. Department of Commerce, NOAA Technical Memo. NMFS-AFSC-421, 398 p.

Napp, J.M., Baier, C.T., Brodeur, R.D., Coyle, K.O., Shiga, N., Mier, K. 2002. "Interannual and decadal variability in zooplankton communities of the southeast Bering Sea shelf." *Deep-Sea Research Part II: Topical Studies in Oceanography* 49(26): 5991-6008.

Nelson, R.J., Carmack. E.C., McLaughlin, F.A., and Cooper, G.A. 2009. "Penetration of Pacific zooplankton into the western Arctic Ocean tracked with molecular population genetics." *Marine Ecology Progress Series* 381:129-138

NOAA. 2008. "Endangered Fish and Wildlife; Final Rule To Implement Speed Restrictions to Reduce the Threat of Ship Collisions With North Atlantic Right Whales." Federal Register v73 no198 p60179.

NOAA. 2013. "Endangered Fish and Wildlife; Final Rule To Remove the Sunset Provision of the Final Rule Implementing Vessel Speed Restrictions To Reduce the Threat of Ship Collisions With North Atlantic Right Whales." Federal Register v78 no236 p73726.

NOAA (National Oceanic and Atmospheric Administration) Fisheries. 2021. NORTH ATLANTIC RIGHT WHALE (*Eubalaena glacialisi*). Accessed 13 June 2022. Available online: https://media.fisheries.noaa.gov/2022-08/N%20Atl%20Right%20Whale-West%20Atl%20Stock_SAR%202021.pdf

Ohashi, R., Yamaguchi, A., Matsuno, K., Saito, R., Yamada, N., Iijima, A., Shiga, N., and Imai, I. 2013. "Interannual changes in the zooplankton community structure on the

southeastern Bering Sea shelf during summers of 1994-2009." *Deep-Sea Research II* 94: 44-56.

Omura, H., Ohsumi, S., Nemoto, F., Nasu, K., and Kasuya, T. 1969. "Black right whales in the North Pacific." *Scientific Report of the Whales Research Institute, Tokyo* 21: 1–78.

Pinchuk, A.I., & Coyle, K.O. 2008. "Distribution, egg production and growth of euphausiids in the vicinity of the Pribilof Islands, southeastern Bering Sea, August 2004." *Deep-Sea Research Part II: Topical Studies in Oceanography*. 55: 1792-1800.

R Core Team 2020. "R: A language and environment for statistical computing. R Foundation for Statistical Computing." Vienna, Austria. URL https://www.R-project.org/.

Razouls, C, Descreumaux, N., Kouwenberg, J., and de Bovee, F. 2005-2022. "Biodiversity of marine planktonic copepods (morphology, geographical distribution and biological data." Sorbonne University, CNRS. Available at http://copepodes.obs-banyuls.fr [Accessed April 25 2022]

Record, N.R., Runge, J.A., Pendleton, D.E., Balch, W.M., Davies, K.T.A., Pershing, A.J., Johnson, C.L., Stamieszkin, K., Ji, R., Feng, Z., Kraus, S.D., Kenney, R.D., Hudak, C.A., Mayo, C.A., Chen, C., Salisbury, J.E., and Thompson, C.R.S. 2019. "Rapid climate-driven circulation changes threaten conservation of endangered North Atlantic right whales." *Oceanography* 32(2): 162–169.

Sameoto, D., Cochrane, N., Herman, A. 1993. "Convergence of acoustic, optical, and net-catch estimates of euphausiid abundance: use of artificial light to reduce net avoidance." *Canadian Journal of Fisheries and Aquatic Sciences* 50: 334-346.

Scarff, J.E., 2001. "Preliminary estimates of whaling-induced mortality in the 19th century North Pacific right whale (*Eubalaena japonica*) fishery, adjusting for struck-but-lost whales and

non-American whaling." *Journal of the Cetacean Research and Management* Special Issue 2: 261–268.

Schabetsberger, R., Brodeur, R., Cianelli, L., Napp, J.M., and Swatzman, G.L. 2000. "Diel vertical migration and interaction of zooplankton and juvenile walleye pollock (*Theragra chalcogramma*) at a frontal region near the Pribilof Island, Bering Sea." *ICES Journal of Marine Science* 57: 1283-1296.

Sharp, S.M., McLellan, W.A., Rotstein, D.S., Costidis, A.M., Barco, S.G., Durham, K., Pitchford, T.D., Jackson, K.A., Daoust, P.Y., Wimmer, T., Couture, E.L., Bourque, L., Frasier, T., Frasier, B., Fauquier, D., Roweles, T.K., Hamilton, P.K., Pettis, H., Moore, M.J. 2019. "Gross and histopathologic diagnoses from North Atlantic right whale *Eubalaena glacialis* mortalities between 2003 and 2018." *Diseases of Aquatic Organisms* 135: 1-31.

Shelden, K., Moore, S., Waite, J., Wade, P., & Rugh, D. 2005. "Historic and current habitat use by North Pacific right whales *Eubalaena japonica* in the Bering Sea and Gulf of Alaska." *Mammal Review* 35(2): 129–155.

Siddig, A.A.H., Ellison, A.M., Ochs, A., Villar-Leeman, C., Lau, M.K. 2016 "How do ecologists select and use indicator species to monitor ecological change? Insights from 14 years of publications in Ecological Indicators." *Ecological Indicators* 60: 223-230.

Silber, G.K. and Adams, J.D., 2019. "Vessel operations in the Arctic, 2015–2017." *Frontiers in Marine Science* 6: 573.

Smith, S.L. 1991. "Growth development, and distribution of the euphausiids *Thysanoessa raschii* and *Thysanoessa inermis* in the southeastern Bering Sea." *Polar Research* 10: 461-478.

Smith, S.L. and Vidal, J., 1986. Variations in the distribution, abundance, and development of copepods in the southeastern Bering Sea in 1980 and 1981. *Continental Shelf Research, 5*(1-2): 215-239.

Smith, T., Reeves, R.R, Josephson, E.A., and Lund, J.N. 2012. "Spatial and seasonal distribution of American whaling and whales in the age of sail." *pLoS ONE* 7(4): e34905.

Smith, L.C. and Stephenson, S.R., 2013. "New Trans-Arctic shipping routes navigable by midcentury." *Proceedings of the National Academy of Sciences 110*(13): E1191-E1195.

Søreide, J.E., Leu, E., Berge, J., Graeve, M., and Falk-Petersen, S. 2010. "Timing of blooms, algal food quality, and *Calanus glacialis* reproduction and growth in a changing Arctic." *Global Change Biology*. 16: 3154-3163.

Stabeno, P., Bond, N.A., Kachel, N.B., Salo, S.A., and Schumacher, J.D. 2001. "On the temporal variability of the physical environment over the south-eastern Bering Sea." *Fisheries Oceanography* 10(1): 81-98.

Stabeno, P., Kachel, N., Moore, S., Napp, J., Sigler, M., Yamaguchi, A., and Zerbini, A. 2012a. "Comparison of warm and cold years on the southeastern Bering Sea shelf and some implications for the ecosystem." *Deep-Sea Research Part II* 65-70: 31–45.

Stabeno, P.J., Farley Jr, E.V., Kachel, N.B., Moore, S., Mordy, C.W., Napp, J.M., Overland, J.E., Pinchuk, A.I. and Sigler, M.F., 2012. A comparison of the physics of the northern and southern shelves of the eastern Bering Sea and some implications for the ecosystem. *Deep Sea Research Part II: Topical Studies in Oceanography*, *65*, 14-30.

Stabeno, P., and Bell, S.W. 2019. "Extreme conditions in the Bering Sea (2017-2018): Record-breaking low sea-ice extent." *Geophysical Research Letters* 46: 8952–8959.

Stevenson, D.E. and Lauth, R.R., 2019. “Bottom trawl surveys in the northern Bering Sea indicate recent shifts in the distribution of marine species.” *Polar Biology 42*(2): 407-421.

Stock Assessment Report. 2022. North Atlantic right whale (*Eubalaena glacialis*): Western Atlantic Stock. *2022 Stock Assessment Report*.

Tarrant, A. M., Eisner, L. B., and Kimmel, D. G. 2021. “Lipid-related gene expression and sensitivity to starvation in *Calanus glacialis* in the eastern Bering Sea.” *Marine Ecology Progress Series* 674: 73-88.

Thorson, J.T. 2019. “Measuring the impact of oceanographic indices on species distribution shifts; The spatially varying effect of cold-pool extent in the Bering Sea.” *Limnology and Oceanography* 64(6): 2632–2645.

Thorson, J.., Adams, C.F., Brooks, E.N., Eisner, L.B., Kimmel, D.G., Legault, C.M., Roger, L.A., and Yasumiishi, E.M. 2020. “Seasonal and interannual variation in spatio-temporal models for index standardization and phenology studies.” *ICES Journal of Marine Science* 77(5) 1879-1892.

Van der Hoop, J.M., Vanderlaan, A.S.M., Cole, T.V.N., Henry, A.G., Hall, L., Mase-Guthrie, B., Wimmer, T., and Moore, M.J. 2014. “Vessel strikes to large whales before and after the 2008 ship strike rule. *Conservation Letters* 8(1): 24-32.

Vidal, J., & Smith, S.L. 1986. “Biomass, growth, and development of populations of herbivorous zooplankton in the southeastern Bering Sea during spring.” *Deep-Sea Research Part A. Oceanographic Research Papers* 33(4): 523-556.

Wade, P., Kennedy, A., LeDuc, R., Barlow, J., Carretta, J., Shelden, K., et al. 2011a. “The world’'s smallest whale population?” *Biology Letters* 7: 83–85.

Wade, P. De Robetis, A., Hough, K.R., et al. 2011b. “Rare detections of North Pacific right whales in the Gulf of Alaska, with observations of their potential prey.” *Endangered Species Research* 13(2): 99–109.

Wang, S.W., Budge, S.J., Iken, K., Gradinger, R.R., Springer , A.M., and Wooller, M.J. 2015. “Importance of sympagic production to Bering Sea zooplankton as revealed from fatty acid carbon stable isotope analyses.” *Marine Ecology Progress Series* 518: 31–50.

Wright, D.L., C.L. Berchok, J.L. Crance, and P.J. Clapham. 2019. “Acoustic detection of the critically endangered North Pacific right whale in the northern Bering Sea.” *Marine Mammal Science*. 35(1): 311–326.

Wright, D.L.; D. Kimmel; N. Roberson; D. Strausz. 2023. “Joint species distribution modeling reveals a changing prey landscape for North Pacific right whales on the Bering shelf.” *Dryad, Dataset*, https://doi.org/10.5061/dryad.hqbzkh1nn.

Wyllie-Eheverria, T., and Wooster, W.S. 1998. “Year-to-year variations in Bering Sea ice cover and some consequences for fish distributions.” *Fisheries Oceanography* 7(2): 159–170.

Zerbini, A.N., Baumgartner, M.F., Kennedy, A.J., Rone, B.K., Wade, P.R., and Clapham, P.J. 2015. “Space use patterns of the endangered North Pacific right whale *Eubalaena japonica* in the Bering Sea.” *Marine Ecology Progress Series*. 532: 269–281.

970 Table 1. Environmental variables used in model fitting of DI growth (rho model) and movement
971 (beta model) terms, ordered alphabetically. Note that DI growth and movement terms are
972 computed independently in the model. The full list of potential variables is listed in Appendix
973 S1: Table S2.

Label	Variable	Model	Resolution of data	Resolution in model	Data source
AL	Aleutian Low (Nov-Mar)	beta	CI	CI	BCW[#]
BT	Bottom Temperature (°C)	rho	Tow	80 km GS	AFSC*
iDm	Days with Ice > 15 March (# days)	beta	25 km cell	80 km GS	NSIDC[%]
IE	Ice extent (km^2)	beta	BS	BS	BCW[#]
Lat	Latitude	beta	GC	80 km GS	ArcGIS Pro
NWs	Northwesterly winds–- summer (May-Sep) (%)	beta	0.25°cell	80 km GS	ERA5[^]
NWw	Northwesterly winds–- winter (Oct-Apr) (%)	beta	0.25°cell	80 km GS	ERA5[^]
pCP	Percentage of cold pool per grid square (%)	beta	BS	80 km GS	Derived BT
SEs	Southeasterly winds–- summer (May-Sep) (%)	beta	0.25°cell	80 km GS	ERA5[^]
SEw	Southeasterly winds–- winter (Oct-Apr) (%)	beta	0.25°cell	80 km GS	ERA5[^]
ST	Surface Temperature (°C)	rho	CTD cast	80 km GS	AFSC*
WGf	Wind gusts–- fall (Sep-Oct) (# days)	beta	0.25°cell	80 km GS	ERA5[^]
WGs	Wind gusts–- summer (May-Sep) (# days)	beta	0.25°cell	80 km GS	ERA5[^]
WGsp	Wind gusts–- spring (Apr-May) (# days)	beta	0.25°cell	80 km GS	ERA5[^]
WGw	Wind gusts–- winter (Oct-Apr) (# days)	beta	0.25°cell	80 km GS	ERA5[^]

974 CI = Climatological index; GC = Geographic coordinate; BS = Bering shelf; 80 km GS = 80-
975 kilometer grid square; *AFSC = NOAA Alaska Fisheries Science Center; [%]NSIDC = National
976 Snow and Ice Data Center (https://nsidc.org/); [^]ERA5 hourly data fifth generation ECMWF
977 Uwind, Vwind, and wind gusts (European Center for Medium-Range Weather Forecasts,
978 https://cds.climate.copernicus.eu/cdsapp#!/home); [#]Bering Climate Website,
979 https://www.beringclimate.noaa.gov/. Wind gusts were computed with threshold of 10 and 15
980 m/s.

Table 2. Twenty fitted gjamTime models with the lowest Deviance Information Criterion (DIC). DIC provides a metric of model parsimony for the entire zooplankton community. Bold indicates the 'best' model for our study, defined as the model that best predicted copepodite stages of *C. glacialis* (Appendix S1: Figure S5). All models were run in *gjam* (v 2.3.2 Clark et al., 2017; 2020) for 20,000 iterations with a 5,000 burn-in; all models in the table were fit with a wind gust threshold of >15 m/s. The rho model describes DI growth (second term in Equation 2), and the beta model describes movement (defined as environmental effects not modeled to depend on population density; first term in Equation 2). See Table 1 for covariate labels; *Int* = intercept

beta model	**rho model**	**DIC**
~ pCP + IE + WGsp + WGf	~ Int + BT + ST	51,294
~ IE + WGsp + WGf	~ Int + BT + ST	51,479
~ WGsp + WGf	**~ Int + BT + ST**	**51,845**
~ pCP + IE + iDm	~ Int + BT	53,003
~ pCP + IE	~ Int + BT	53,424
~ WGsp + WGf + AL	~ Int + BT + ST	53,434
~ WGsp + WGf	~ Int + BT	54,682
~ pCP + IE	~ Int + BT + ST	54,731
~ pCP + IE	~ Int + BT + ST	54,940
~ pCP + pCP*Lat + Lat + IE + WGsp + WGf	~ Int + BT + ST	55,149
~ IE + WGsp + WGf + iDm	~ Int + BT + ST	55,199
~ pCP + IE + WGsp + WGf	~ Int + BT	55,596
~ pCP + IE + WGf	~ Int + BT + ST	55,970
~ pCP + iDm	~ Int + BT	55,988
~ pCP + IE + WGsp + WGf + NWs + SEs + NWw + SEw	~ Int + BT + ST	56,105
~ pCP + iDm	~ Int + BT + ST	56,377
~ IE + WGsp + WGf	~ Int + BT	56,485
~ pCP + IE + WGsp + WGf + AL	~ Int + BT + ST	56,994
~ IE + Lat	~ Int + BT + ST	57,350
~ pCP + IE + iDm	~ Int + BT + ST	57,447

990 Figure 1. North Pacific right whale sightings in the Bering Sea, 1970 to present. Black pentagon
991 denotes the federally designated Bering Sea right whale critical habitat. Sighting data provided
992 by NOAA Alaska Fisheries Science Center Marine Mammal Laboratory.
993
994 Figure 2. Eastern Bering Sea shelf with zooplankton tows (circles; 2006-2016); closed circles
995 indicate tows used in this study. Yellow grid is the 80 km cell study blocks (*n*=14). Black
996 pentagon denotes the federally designated Bering Sea right whale critical habitat. Bathymetric
997 contour lines presented in 50 m increments from 50 to 2,000 m depth (blue gradient from dark to
998 light). Oceanographic Domains of the shelf include the Inner Domain (0-50 m), Middle Domain
999 (50-100 m), and Outer Domain (100-200 m; Coachman 1986).
1000
1001 Figure 3. Zooplankton community with guilds based on size, stage, and diet. Arrows denote
1002 energy flow (from prey to predator). Shading symbolizes species, sizes, and stages included in a
1003 guild with potential North Pacific right whale prey shaded in color (red = *C. glacialis*; orange =
1004 *Neocalanus* species, and teal = *Thysanoessa* species) and other species shaded in gray; light gray
1005 text indicates sizes and stages missing from dataset. Copepod life history stages develop from
1006 copepodite stage 1 (C1) to copepodite stage 5 (C5) followed by C6 (referred to as 'Adults' in the
1007 text).
1008
1009 Figure 4. Contributions to dynamics in zooplankton species assemblage; brown = density-
1010 dependence, light blue = density-independent growth, and dark brown = movement. Upper plot
1011 shows the proportion of variance explained for each component and lower plot shows standard
1012 deviations for the three contributions on the observed scale (zooplankton data were fourth root

transformed). Colored circles below the upper plot correspond to potential North Pacific right whale prey species (red = *C. glacialis*; orange = *Neocalanus* species, and teal = *Thysanoessa* species).

Figure 5. Posterior parameter estimates for zooplankton species abundance to (A) bottom temperature (°C**,** BT) and surface temperature (°C**,** ST) in matrix $\boldsymbol{\rho}$ (rho; density-independent growth; Equation 2) and (B) # of days with wind gusts >15 m/s from spring (WGsp; Apr-May) and fall (WGf; Sep-Oct) in matrix $\boldsymbol{\beta}$ (beta; movement term; Equation 2). Colors correspond to species (red = *C. glacialis*; orange = *Neocalanus* species; teal = *Thysanoessa* species; gray = other species). Circles denote median and lines bound 95% of the posterior distribution. Species ordered by guild (microzooplankton predator [M.], small omnivore, small-med omnivore, large omnivore, predators, and epibenthic [Epiben.]; Figure 2).

Figure 6. Predicted equilibrium abundances (**w***) of *Calanus glacialis* along a gradient in bottom water temperature (zero-centered +/- two SDs) for a model output with (A) movement terms, spring and fall wind gusts and DI growth terms, bottom and surface temperature, and (B) only DI growth terms. Thick bars bound 68% and thin bars bound 95% predictive intervals. Note that **w*** is on the model output scale (fourth root transform of ind. m^{-3}).

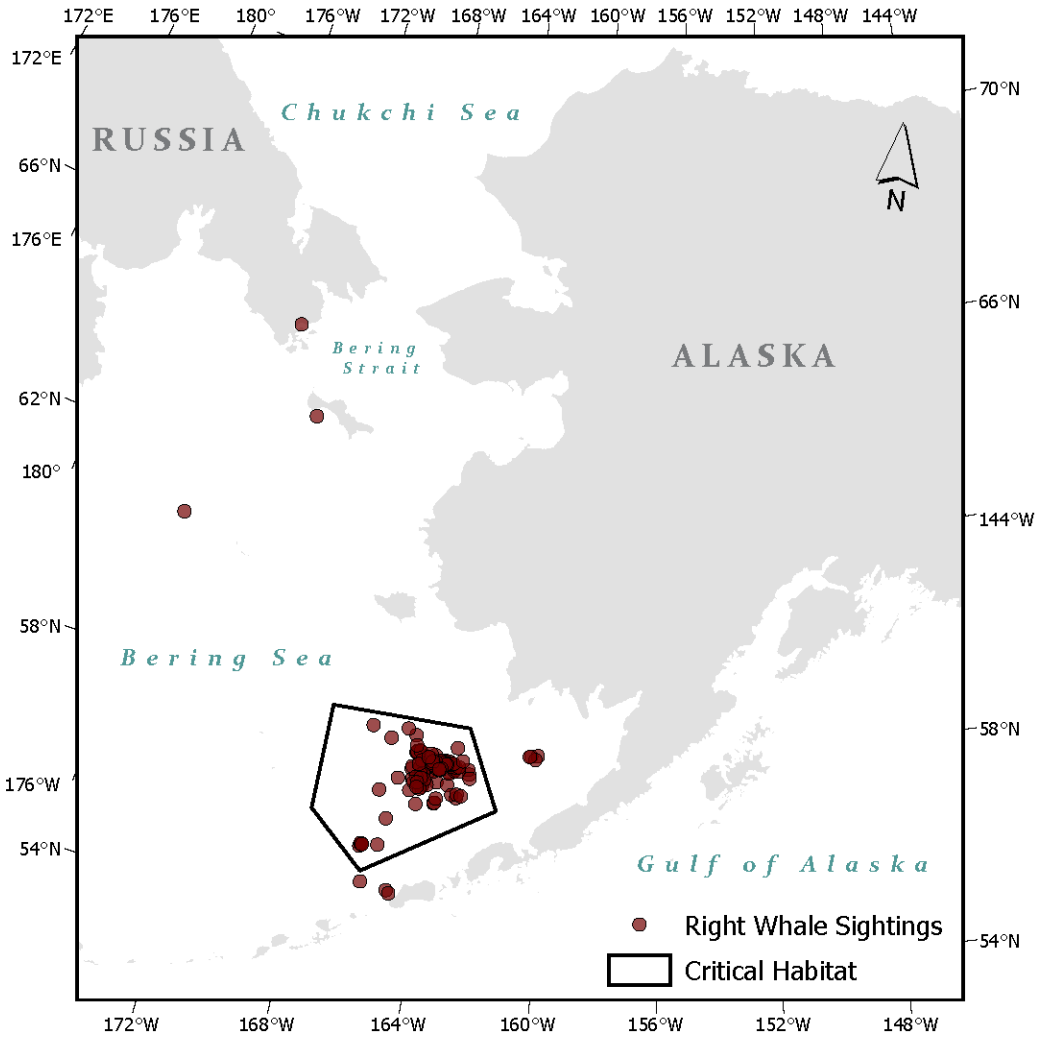

1032

1033 Figure 1.

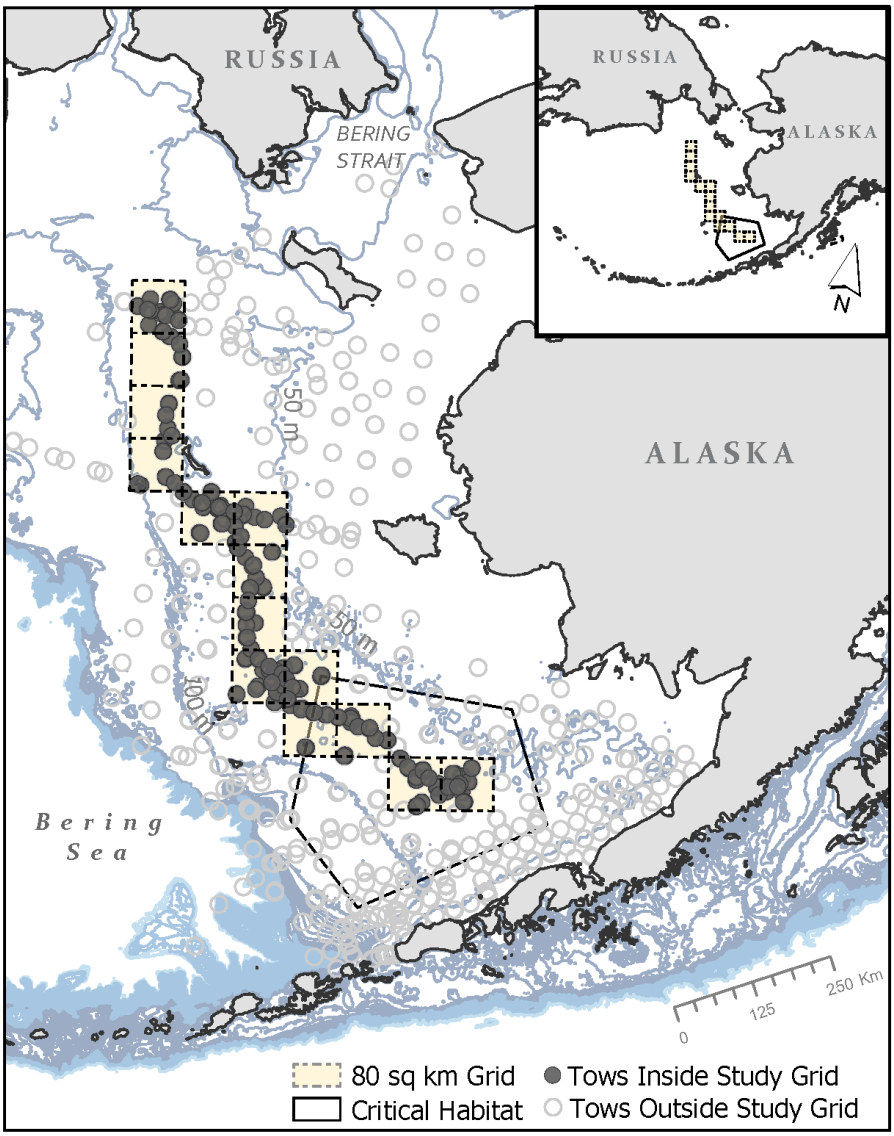

1034

1035 Figure 2.

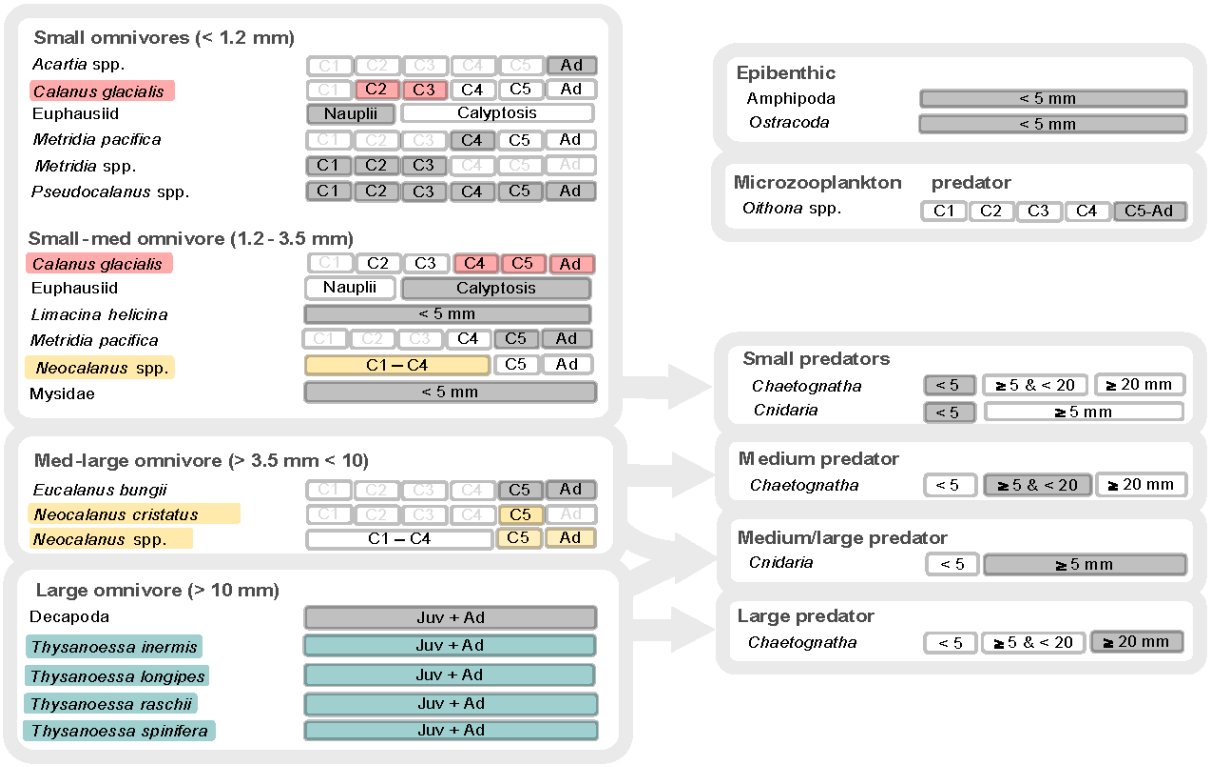

1036

1037 Figure 3.

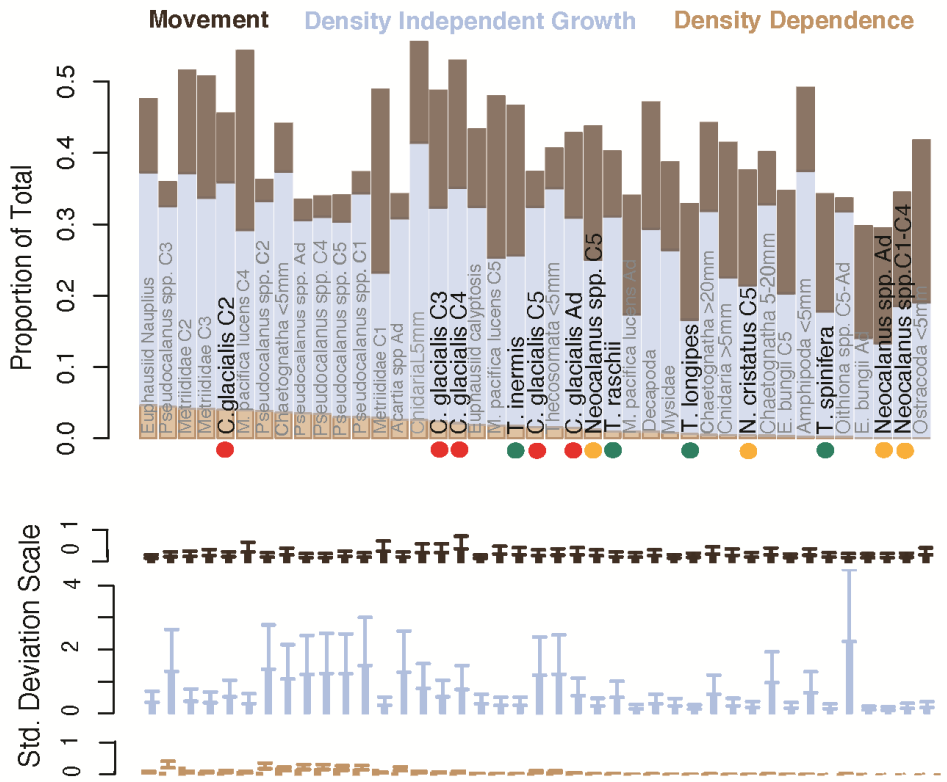

1038

1039 Figure 4.

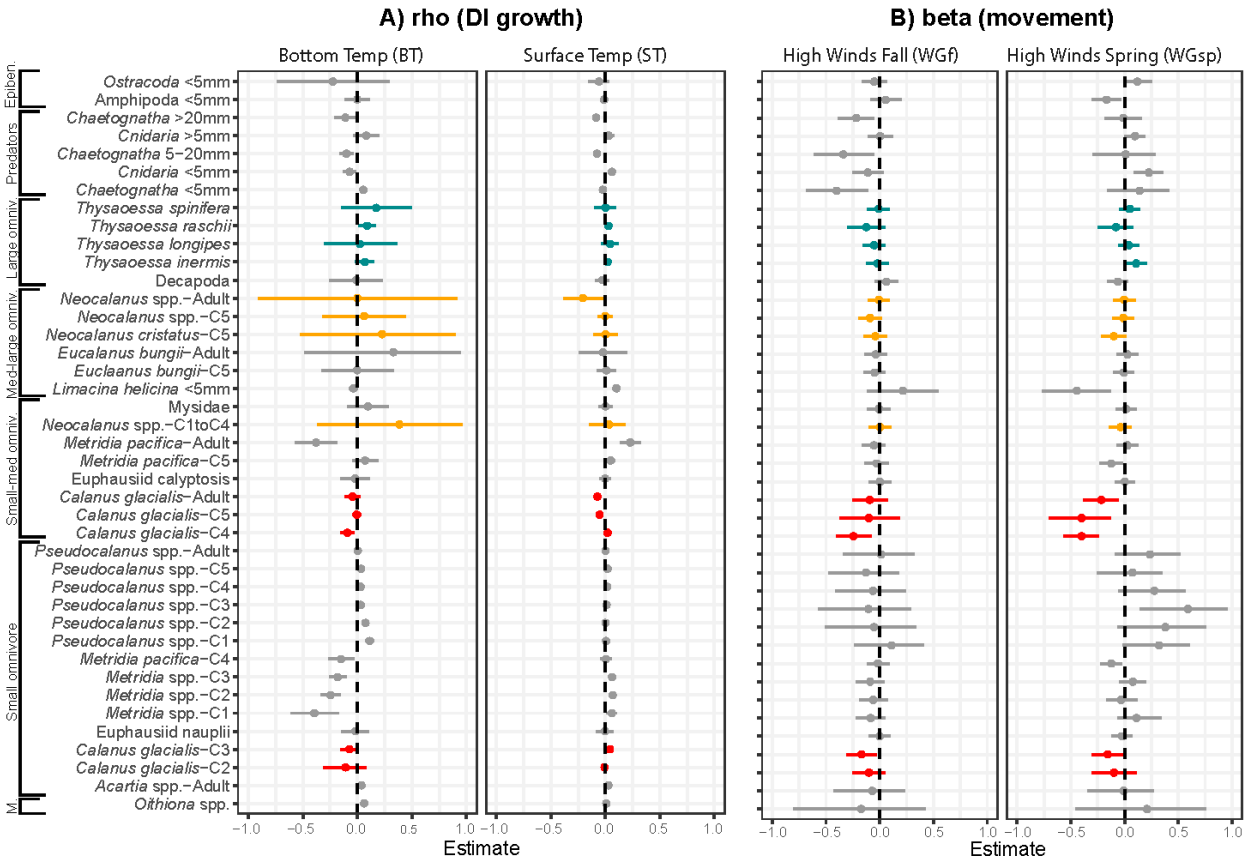

1040

1041 Figure 5.

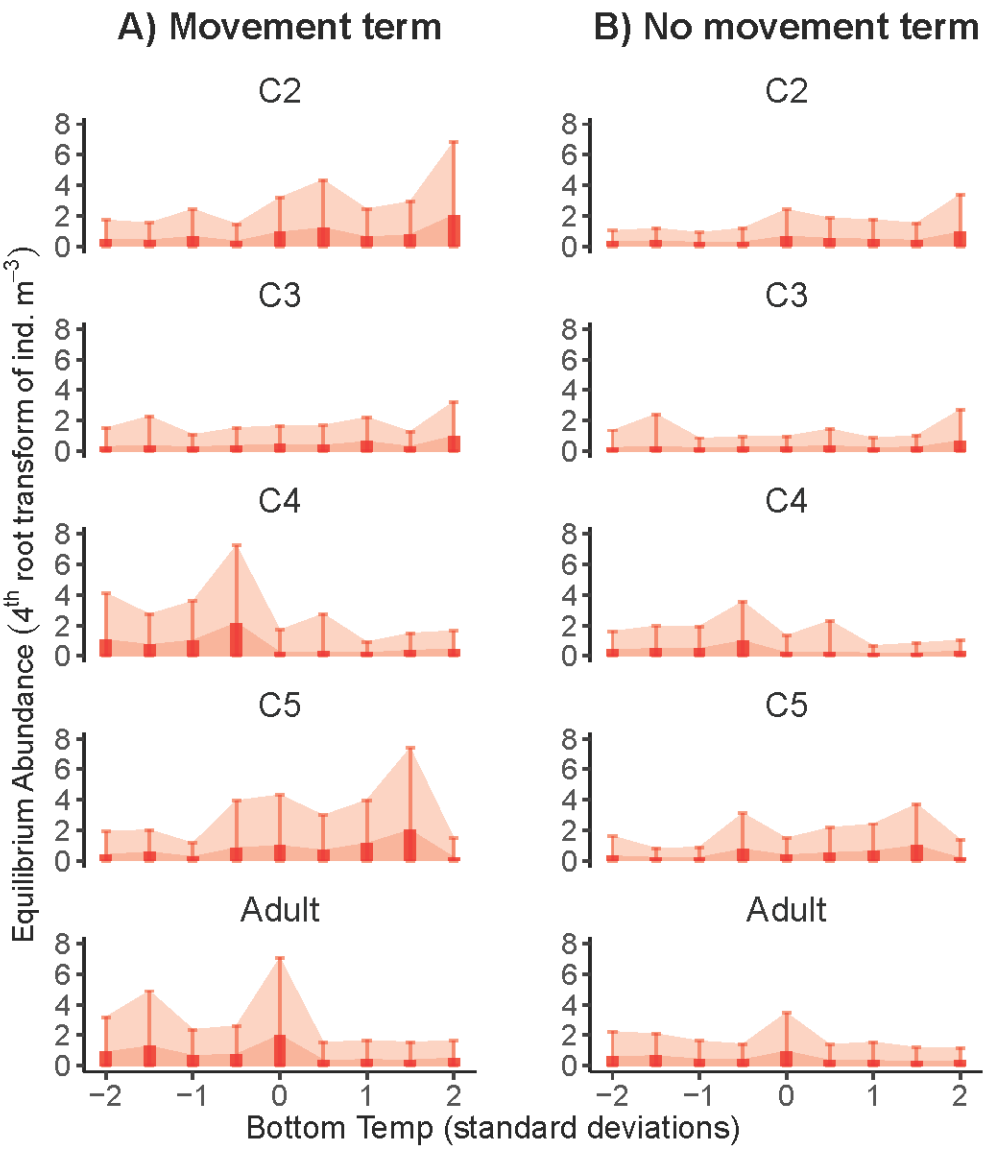

1042

1043 Figure 6.